

VTT PUBLICATIONS 341

# **Unidirectional JMC actuators and their approximations in the active attenuation of noise in ducts**

Seppo Uosukainen  
VTT Building Technology

Vesa Välimäki  
Helsinki University of Technology,  
Laboratory of Acoustics and Audio Signal Processing



---

TECHNICAL RESEARCH CENTRE OF FINLAND  
ESPOO 1998

ISBN 951-38-5223-7 (nid.)

ISSN 1235-0621 (nid)

ISBN 951-38-5224-5 (URL: <http://www.inf.vtt.fi/pdf/>)

ISSN 1455-0849 (URL: <http://www.inf.vtt.fi/pdf/>)

Copyright © Valtion teknillinen tutkimuskeskus (VTT) 1998

#### JULKAISIJA – UTGIVARE – PUBLISHER

Valtion teknillinen tutkimuskeskus (VTT), Vuorimiehentie 5, PL 2000, 02044 VTT  
puh. vaihde (09) 4561, faksi (09) 456 4374

Statens tekniska forskningscentral (VTT), Bergsmansvägen 5, PB 2000, 02044 VTT  
tel. växel (09) 4561, fax (09) 456 4374

Technical Research Centre of Finland (VTT), Vuorimiehentie 5, P.O.Box 2000, FIN-02044 VTT, Finland  
phone internat. + 358 9 4561, fax + 358 9 456 4374

VTT Rakennustekniikka, Rakennusfysiikka, talo- ja palotekniikka, Lämpömiehenkuja 3, PL 1804, 02044 VTT  
puh. vaihde (09) 4561, faksi (09) 456 4709

VTT Byggnadsteknik, Byggnadsfysik, hus- och brandteknik, Värmemansgränden 3, PB 1804, 02044 VTT  
tel. växel (09) 4561, fax (09) 456 4709

VTT Building Technology, Building Physics, Building Services and Fire Technology,  
Lämpömiehenkuja 3, P.O.Box 1804, FIN-02044 VTT, Finland  
phone internat. + 358 9 4561, fax + 358 9 456 4709

Technical editing Kerttu Tirronen

Oy EDITA Ab, ESPOO 1998

Uosukainen, Seppo & Välimäki, Vesa. Unidirectional JMC actuators and their approximations in the active attenuation of noise in ducts. Espoo 1998, Technical Research Centre of Finland, VTT Publications 341. 88 p. + app. 12 p.

**UDC** 681.586:534.83:621.643

**Keywords** ducts, noise reduction, acoustic waveguides, unidirectional actuators, sound transmission

## Abstract

This report deals with a fundamental problem of feedforward active noise control systems in ducts, the acoustic feedback from the canceling actuator to the reference detector. A natural solution to this problem is to use a unidirectional actuator. The starting point of this study is the JMC source that is an ideal unidirectional actuator but is difficult to realize. Potential unidirectional *three-element* actuator systems are surveyed systematically by modifying and approximating the JMC source in various ways. As a result, one realizable ideal unidirectional three-element source configuration and four nearly unidirectional approximations of it are discovered. Also *two-element* unidirectional JMC actuators are handled, in which the elements act as a dipole with the monopole effect included in the same elements. As a result, one ideal unidirectional two-element solution and six approximations of it are found. The inter-channel delay in the control structure of the two-element actuators is optimized so that the residual sound pressure downstream or upstream from the unidirectional source will be minimized, or the delay is omitted altogether. The two-element ideal solution and its approximations are derived for each three ways of handling the delay. The output volume velocities of all the three variations of two-element Ideal Source are mutually identical and independent of the inter-channel delay optimization, and are also identical with those of Swinbanks' two-element actuator, although the procedure of attaining them is quite different. Especially the delayless version of two-element Ideal Source has the advantage of no separate phase shift between the volume velocities of the elements, which turns out to be advantageous in the practical implementation of digital control systems. Using the unidirectional solutions with no inter-channel delays makes it possible to achieve simplified control algorithms and reduce the computing time or improve the performance. Digital control of some of the structures and their practical limitations are considered. Examples of realizable digital control systems are given.

# Preface

The work described in this report has been conducted as a part of a Finnish project on active noise control, AKTIVA, during the years 1995 – 1997. The project was financed by TEKES and Finnish companies that have interest in the application of modern methods for noise control. This collaboration between VTT and Helsinki University of Technology, Laboratory of Acoustics and Audio Signal Processing, has been made possible by Mr. Hannu Nykänen (VTT Manufacturing Technology) who was the coordinator of the AKTIVA project. Vesa Välimäki, the second author of this report, worked for the AKTIVA project from August 1996 until December 1997. His responsibilities included design and implementation of digital active noise control systems.

The authors are grateful to their colleagues Dr. Jukka Linjama (VTT Manufacturing Technology), Mr. Marko Antila (VTT Manufacturing Technology), Mr. Seppo Rantala (VTT Automation), and Mr. Ari Saarinen (VTT Building Technology) for helpful discussions on unidirectional actuator systems. Ms. Leila Uosukainen has revised the language of this work.

Espoo, January 1998

Seppo Uosukainen (e-mail: [Seppo.Uosukainen@vtt.fi](mailto:Seppo.Uosukainen@vtt.fi)) &  
Vesa Välimäki (e-mail: [Vesa.Valimaki@hut.fi](mailto:Vesa.Valimaki@hut.fi))

# Contents

Abstract	3
Preface	4
List of symbols	8
1. Introduction	11
1.1 General	11
1.2 Two-element unidirectional actuators	13
1.3 Three-element unidirectional actuators that are not based on the JMC method	13
1.4 Actuators with more than three elements	14
1.5 Actuators based on the JMC method	15
1.6 Purpose of this report	16
2. Basic physical constructions	19
2.1 Basic three-element construction	19
2.2 Basic two-element construction	21
3. Well-known unidirectional solutions	22
3.1 Three-element solution according to the JMC method	22
3.2 Two-element solutions	22
3.2.1 Swinbanks' solution	23
3.2.2 Maximally efficient source	25
4. New solutions based on the JMC method	28
4.1 New three-element solutions	28
4.1.1 Basic solution	28
4.1.2 Modified solution	28
4.1.3 Ideal Source and four approximations	29
4.1.4 Weighting functions	30
4.1.5 Delay realization of the weightings	31
4.1.6 Residual sound pressures	32
4.2 New two-element solutions	32
4.2.1 Basic solution	33

4.2.2 Modified solution with three choices of inter-channel delay optimization	34
4.2.3 Ideal Source and six approximations	36
4.2.4 Weighting functions	37
4.2.5 Delay realization of the weightings	38
4.2.6 Residual sound pressures	41
5. Comparison of the new unidirectional solutions	45
5.1 Three-element solutions	45
5.1.1 Weighting functions	45
5.1.2 Residual sound pressures	46
5.2 Two-element solutions	48
5.2.1 Weighting functions	49
5.2.1.1 Two-element Ideal Source	49
5.2.1.2 Approximation 6	49
5.2.1.3 Approximations 7 and 8	52
5.2.1.4 Approximations 9 and 10	53
5.2.2 Residual sound pressures	54
5.2.2.1 Approximation 5	55
5.2.2.2 Approximations 7 and 8	57
5.2.2.3 Approximations 9 and 10	57
5.3 Concluding remarks on the continuous available frequency bands	59
6. Digital control of unidirectional actuator systems	62
6.1 Digital filter approximation of frequency-dependent weightings	62
6.1.1 Design example: weighting filter b for Approximations 3 and 4	64
6.2 Digital integrator	65
6.2.1 Recursive feedback loop and FIR compensator	65
6.2.2 Combined approximation of the integrator and the dipole weighting	68
6.2.3 Design example: three-element Ideal Source	68
6.3 Digital implementation of time delays	70
6.3.1 Propagation delay	70
6.3.2 Delay between actuator elements in two-element systems	71
6.3.3 Delay $\tau/2$ in the control of the dipole control path in two-element systems	72

6.4 Design examples of two-element actuators	73
6.4.1 Two-element Swinbanks' source	73
6.4.2 Delayless two-element Ideal Source	76
6.5 Implementation issues	79
6.6 Discussion of digital control	80
7. Conclusions	81

## APPENDICES

- Appendix A: Derivations of frequency-dependent weighting functions for the three-element JMC actuators
- Appendix B: Derivations of frequency-dependent weighting functions for the two-element JMC actuators

## List of symbols

$A$	amplitude factor in Swinbanks' two-element actuator with a separate integrator
$a$	dipole weighting
$a_1$	coefficient in $I(z)$
$B_1(z)$	transfer function of the FIR compensator in $I(z)$
$b$	monopole weighting
$c$	ratio of upstream to downstream sound pressures
$c_0$	speed of sound of a fluid at rest
$c_1$	limiting ratio of incoming to upstream sound pressures
$c_2$	limiting ratio of incoming to downstream sound pressures
$D$	scaled delay $\tau/T$
$d$	distance between outermost actuator elements
$F_d$	frequency response of an allpass fractional filter for a delay of $\tau$
$f_s$	sampling frequency
$h_b(i)$	coefficients for a FIR filter approximation of $b$ , $i = 0, 1, 2, \dots$
$I(z)$	transfer function of a scaled digital integrator according to equation (22)
$j$	imaginary unit

$k$	wave number ( $\omega/c_0$ )
$L$	distance between the detector and the middle of the actuator unit
$L_{\text{FIR}}$	length of FIR filter
$n$	integer number
$p_i$	incoming sound pressure at the middle of the actuator unit
$p_L$	incoming sound pressure at the detector
$p_+$	sound pressure radiated by the actuator unit downstream
$p_-$	sound pressure radiated by the actuator unit upstream
$q_i$	volume velocity related to $p_i$ according to equation (1)
$q_L$	volume velocity related to $p_L$ similarly as defined for $q_i$
$q_0$	volume velocity of the actuator element in the middle (in three-actuator systems)
$q_1$	volume velocity of the first actuator element
$q_1$	volume velocity of the last actuator element
$r$	order of the feedback part
$S$	cross-sectional area of the duct
$T$	sampling interval
$W$	WLS weighting function
$x$	Cartesian co-ordinate

$z$	complex variable used in Z-transforms
$\lambda$	wavelength of sound
$\rho_0$	density of fluid at rest
$\tau$	propagation acoustic delay between the outermost actuator elements
$\tau_L$	propagation acoustic delay between the detector and the middle of the actuator unit
$\omega$	angular frequency $2\pi f$ , where $f$ is frequency
$\text{Re}\{\cdot\}$	real part
$\text{Im}\{\cdot\}$	imaginary part
$\hat{a}$	frequency response of the digital filter approximation of $a$ , same notation used also for $b$ and $I$

# 1. Introduction

## 1.1 General

Active noise control (ANC) in ducts is an important field of research. One reason for the great interest in the active control of sound in ducts is that the sound field is one-dimensional at low frequencies, that is, sound propagates in two directions only and the problem is thus relatively easy. Another reason is that this particular area of ANC has a large range of commercial applications, such as attenuation of noise in air-conditioning systems and in exhaust pipes of engines. Doak [1, 2] has described the practical and theoretical background to, and principal features of, the theory of acoustic fields caused by source distributions in ducts of finite length.

Control for the actuator, used as an anti-noise source (secondary source), can be obtained from either the original or silenced noise. In the first case one talks about feedforward control, in the second about feedback control, see, e.g., [3]. Feedback control can in some circumstances become unstable, and in principle the realization of feedforward control is easier. In duct applications, the reference detector in feedforward control is normally mounted before the actuator with respect to the direction of sound propagation; in feedback control the reference detector is normally mounted adjacent to or after the actuator.

For true feedforward control to work, it is required that the actuator in the duct radiates only in the direction of sound propagation, i.e., downstream [4]. Normally an actuator radiates also in the opposite direction (upstream) causing an *acoustic feedback* from the secondary source to the reference detector. The acoustic feedback may interfere with the operation of the control system and even render it unstable. It also causes an increase in the noise level upstream of the canceling source. It is thus a principal problem in feedforward active noise control in ducts.

The effect of the acoustic feedback can be minimized by several alternative methods. Of course, the easiest way of eliminating it totally is to use a non-acoustic reference signal, obtained, e.g., with a tachometer installed on the noise source. This is not always possible, e.g., in cases when the noise source has a

wideband spectrum. One possibility of minimizing the acoustic feedback is to use adaptive filters [5, 6], especially adaptive IIR filters [7]. This presumes a more complicated control system. The minimization can be realized by using electronic feedback to compensate the acoustic feedback with, e.g., Chelsea monopole or the tight-coupled monopole [8, 9] or other constructions [10]. This method presumes exact phase responses of the system, probably varying with the thermodynamic circumstances. The feedback can also be suppressed by installing the detector microphone between two monopole-type actuator elements radiating in antiphase causing the effect of the actuator to be eliminated from the reference signal, the construction being called Chelsea dipole [11]. Moreover, a dual sensing microphone [12] can be used. In this solution the reference and error microphones are at an equal distance on opposite sides from the (monopole) actuator. The error microphone signal is subtracted from the reference signal, the effect of the actuator thus being eliminated from the reference signal. The last three methods are sensitive to errors in the placement of the microphones. Also, if the attenuation is not complete (which is the case in practice), there is always error in the manipulated reference signal in the last method.

All the mentioned feedback minimization methods have the property that they do not eliminate the upstream radiation of the actuator but only suppress its effects on the control system. Geometrical arrangement of the secondary source configuration, e.g., a tree-shaped configuration [13], can be used to minimize the radiation of the secondary sound wave upstream. This method does not lead to an ideally unidirectional system, however.

The most natural technique to suppress the acoustic feedback and upstream radiation is the use of unidirectional actuators, unidirectional detectors, or both simultaneously. With a unidirectional actuator or detector the control system can be kept relatively simple [14]. Unidirectional systems are constructed of several actuator or detector elements. This may be seen to be a drawback, but also in other cases, e.g., when higher order modes are taken into account, several elements are needed. The distance of the actuator or detector elements determines an upper frequency limit to the functioning of the system. Thus the systems have limited frequency ranges, which fortunately can be selected by a proper choice of the distance. On the other hand, all other solutions have also

limited frequency ranges, e.g., all digital systems are functioning only at frequencies below their Nyquist frequencies.

## **1.2 Two-element unidirectional actuators**

Swinbanks [15] has described an ideal two-element unidirectional solution where the upstream radiation is eliminated by introducing a delay for the first actuator, corresponding to the acoustic propagation delay between the two actuators, and feeding the actuators in opposite phases. The first actuator is situated upstream from the second one. The improper frequency response is compensated by inverse filtering. Poole and Leventhall [16] have verified Swinbanks' work by experiment.

Based on Swinbanks' work, Berengier and Roure [17] have proposed a positive feedback loop with a delay to the input of the actuators, thus avoiding extra frequency response equalization. From the three-element solution of Swinbanks, the same feedback loop for the two-element solution can also be deduced. Winkler and Elliott [14] use the acoustic propagation delay between the two actuators but applied to the second actuator, and feed the actuators otherwise in the same phase. This solution is called the "maximally efficient source". It refers to a source eliminating the total sound pressure downstream with least "effort" [3]. The least effort signifies minimizing the square of the absolute values of the volume velocities of the source complex. The maximally efficient solution is not unidirectional at low frequencies.

## **1.3 Three-element unidirectional actuators that are not based on the JMC method**

In principle, two actuator elements are enough for a unidirectional acoustic source in a duct. That is why many three-element solutions are based on extra requirements on the system (in addition to unidirectionality and total sound elimination downstream). Swinbanks [15] uses different distances between the actuators, and optimizes by trial the distances (and corresponding delays) and the magnitudes of the elements to obtain as large a useful frequency range as possible. The output of the first actuator element is the combination of two

components: the first component is the delayed negative version of the output of the second actuator element and the second component is the delayed negative version of that of the third actuator element, the delays corresponding to the acoustic propagation delays between the corresponding actuator elements. The outputs of the second and third actuator element are the same, the latter being delayed by the acoustic propagation delay between those elements. The presented properties of the system make it unidirectional. The improper frequency response is compensated by a suitable equalization.

Swinbanks also explains how the frequency response equalization can be replaced by two positive feedback loops with delays. Based on Swinbanks' work, Berengier and Roure [17] use inter-channel delays and the frequency response equalization is replaced by positive and negative feedback loops with delays. The first two actuator elements are delayed with respect to the third actuator element, corresponding the acoustic propagation delays between them. Otherwise the system parameters are made unequivocal by an extra requirement of stationarity of the upstream field with respect to variations of flow and sound velocities. Since the extra requirement of Berengier and Roure is different from that of Swinbanks, the feedback loops for the frequency response equalization are not similar. La Fontaine and Shepherd [18] use in their experimental work the same inter-channel delays as Berengier and Roure with equally spaced elements and the frequency response equalization is realized by a transversal filter. The tap weights of the filter are determined by minimizing the sum of the squares of the proportional errors, where the error designates the difference between the desired frequency response and the actual frequency response realized by a filter with a stepwise continuous impulse response, at predestined frequencies.

## **1.4 Actuators with more than three elements**

The purpose of using more actuators is to obtain better properties of the actuator system, e.g., wider frequency range, better low-frequency radiation properties etc. The three-element solutions of Swinbanks [15] and Berengier and Roure [17] can be readily generalized to multi-element versions. Kazakia [19] suggests using four elements in the actuator, in order to obtain a more efficient radiator at low frequencies. Otherwise his principle of selecting the system parameters is

the same as with Swinbanks' three-element system. Eghtesadi and Leventhall [20] also use the same inter-channel delays as the multi-element generalization of Swinbanks' solution, with equally spaced elements. The first  $n - 1$  elements have the same magnitudes, their sum being the same as the magnitude of the last element. Despite the inter-channel delays, the first  $n - 1$  elements are in anti-phase with the first one. Guicking and Freienstein [21] have found that similar results as with an array of  $n$  equidistant sources can be obtained with a thinned array where certain sources are omitted.

## 1.5 Actuators based on the JMC method

The *JMC method* is suitable for formulating the problem of active noise control with the general system theory, although the method can be applied more generally to reshaping of acoustic fields [22, 23, 24, 25, 26, 27]. Its name originates from the first three pioneers of the method: Jessel, Mangiante, and Canévet [24]. A generalized JMC method has been proposed by Mangiante [28]. Furthermore, a modified JMC method has been introduced by Uosukainen [29]. Generally, three types of secondary sources are needed in the method—namely monopole, dipole and quadripole source distributions. In the case of duct applications (with a plane wave mode), the quadripole distributions vanish. In addition, magnitudes of partial sound fields in the main lobe, caused by monopole and dipole distributions, are equal, so the radiation pattern of an actuator element is a cardioid. An ideal actuator combination in the JMC method radiates only in one direction in the duct, so no radiation upstream exists. An ideal actuator also totally eliminates the original sound field downstream. This ideal actuator thus consists of an ideal monopole and an ideal dipole.

Jessel, Mangiante, and Canévet [30, 31, 32, 28] use a combination of a monopole and dipole radiator, having coincident acoustic centers with respect to the direction of sound propagation, to obtain a three-element unidirectional source according to the JMC method. In the realizations of the systems, the dipole radiator is approximated by two closely situated monopoles. The propagation delay from the detector to the actuator and the improper frequency response are compensated by delays and equalization, tuned experimentally. La Fontaine and Shepherd [18] state that this system has disadvantages compared to Swin-

banks' arrangements, due to the need of a balanced three-loudspeaker system and a phase shift of  $90^\circ$  in the system.

Formerly, there have not appeared presentations of two-element unidirectional actuators that are based on the JMC method in literature.

## 1.6 Purpose of this report

All the unidirectional actuator systems presented above, except for the solutions based on the JMC method, need inter-channel delays in their control systems. In digital control systems, the accurate realization of short delays requires much signal processing power. This fact supports the use of the JMC method, to achieve simplified control algorithms, reduce the computing time, and improve the performance [28]. In addition, the JMC method is purely an exact field-theoretical approach to the problem of field reshaping, so it always yields the optimum solution to any field reshaping problem. From this point of view it is a very natural starting point. That is why the JMC method has been adopted by the authors.

There is no systematic presentation of the realization of JMC actuators. Especially the two-element versions do not appear in literature. This speaks in favour of a thorough presentation to be delivered. The starting point of this study is the JMC source that is an ideal unidirectional actuator but is difficult to realize. Potential unidirectional actuator systems are surveyed systematically by modifying and approximating the JMC source in various ways. This report deals with unidirectional three- and two-element JMC actuators and their approximations. As new three-element solutions, one ideal source and four approximations are presented. As new two-element solutions, one ideal source and six approximations are presented with three different inter-channel delays (one solution with one inter-channel delay corresponds the maximally efficient source of Winkler and Elliott [14]).

In order not to cause hindrance to possible flow in the duct, the actuator elements are best mounted at the walls of the duct. This prevents the use of pure dipole actuator elements, so the dipoles must be realized by two monopoles near each other. Of course the use of monopole elements only makes the system an

approximation, but fortunately the nonidealities can be corrected by proper frequency-dependent magnitude weightings of the elements.

The JMC element can be realized also by two monopole-type actuator elements only. The two-element actuators are fed so that they produce both the monopole and dipole parts of radiation, approximately or exactly, in order to produce similar sound fields as the JMC source. Similar approach has been used by Boone and Ouweltjes [33] to obtain a loudspeaker system with a cardioidlike radiation pattern in a three-dimensional space. Elliott [34] has used two closely spaced microphones in a tube to measure the incident and reflected travelling wave components to evaluate the absorption coefficient of a sample placed at the end of the tube. His construction leads to similar control systems as with one of our two-element solutions but without any weighting functions.

The monopole part of the two-element actuators is phased so that the monopole radiation is correct (1) downstream or (2) upstream, or (3) with no inter-channel delay at all. The choice of best delay optimization is not obvious because optimal functioning in one direction may lead to unsatisfying performance in the other direction. The delay optimization also affects the weighting filters of the actuators and different choices thus bring about changes in the computational complexity of a digital control structure of the unidirectional sources.

With two-element JMC actuators, there is a need to have a frequency-response equalization as with Swinbanks' source. An integrator in the control system is introduced by the authors to the equalization. With the integrator, there is no need to a separate phase shift of  $90^\circ$  in any system considered. Therefore also the disadvantages stated by La Fontaine and Shepherd [18] are eliminated.

Evidently the frequency responses of the actuator elements, both magnitude and phase, have to be equalized, in order to obtain tolerably similar frequency responses from the elements. This is necessary for the system to be able to work unidirectionally. This equalization may be realized adaptively or with fixed filters that will be adjusted according to measurements. These aspects are beyond the scope of this report and may be handled in forthcoming papers.

In this report several assumptions have been made: the frequency is assumed to be low enough so that only plane wave mode is present; the duct is assumed to

be infinitely long, and hence no reflections from either ends of the duct exist; the duct is assumed to be infinitely hard-walled and therefore the impedance of the duct wall is not taken into account; the medium in the duct is assumed to be homogenous and flowless, implying that the sound speed is constant everywhere in the duct and independent of the propagation direction of the sound; the medium is assumed to be ideal fluid, so no viscous or thermal losses are present. The effects of higher order modes, end reflections, duct wall impedance, inhomogenities and losses of the fluid, and flow may be treated in future papers.

This report is organized as follows. In Section 2 the basic three- and two-element unidirectional actuator constructions are presented. Section 3 discusses well-known solutions based on the basic constructions. In Section 4 new solutions based on the basic construction and the JMC method are introduced. With two-element constructions, structures with down- or upstream inter-channel delay optimization or no delay are introduced. In Section 5 these solutions are compared in terms of the obtainable residual sound pressure (both down- and upstream), the magnitude weightings needed in the constructions, and the width of the available frequency range. Implementation of digital control structures for the two-element unidirectional sources is discussed in Section 6. Conclusions are drawn and perspectives for further research in the field are given in Section 7.

## 2. Basic physical constructions

### 2.1 Basic three-element construction

An ideal dipole radiator, having its main lobes in the upstream and downstream directions in the duct, is difficult to realize without causing hindrance to possible flow in the duct. That is why it is expedient to approximate the dipole with two monopoles in opposite phases. Our basic three-element construction to be examined here consists of three actuator elements of monopole type located at  $x = 0$  and  $\pm d/2$  having thus a mutual distance of  $d/2$  as depicted in Figure 1. The outermost monopoles at  $x = \pm d/2$  with the mutual distance of  $d$  form the dipole approximation and the element in the middle at  $x = 0$  acts as the actual monopole element. The corresponding field and source quantities are presented in Figure 2. The dipole elements produce volume velocities  $q_1$  and  $q_2$  while the monopole element produces volume velocity  $q_0$ .

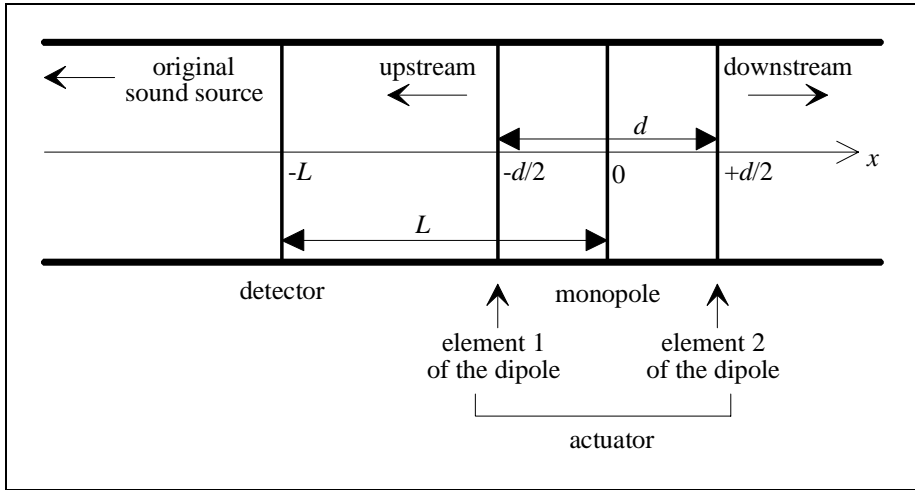


Figure 1. Schematic presentation of the geometry of the three-element actuator construction in a duct.

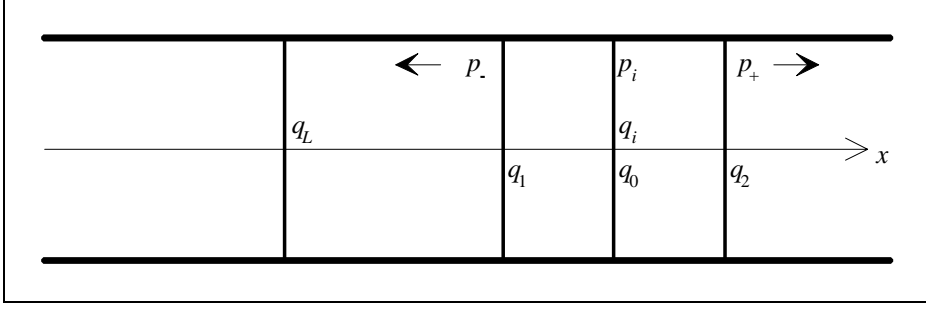


Figure 2. Schematic presentation of the field and source quantities in the three-element actuator construction in a duct.

The quantity  $q_i$  in Figure 2 is related to the original sound pressure  $p_i$  at  $x = 0$  by

$$q_i = \frac{p_i S}{\rho_0 c_0} , \quad (1)$$

where  $S$  is the cross-sectional area of the duct,  $\rho_0$  is the density of the fluid at rest and  $c_0$  is the speed of sound in the fluid. The sound is detected at  $x = -L$ . The relations between the original field quantities at the detector point (subscript  $L$ ) and the origin (middle of the actuator) are

$$\begin{aligned} p_i &= p_L e^{-jkL} \\ q_i &= q_L e^{-jkL} , \end{aligned} \quad (2)$$

where  $j$  is the imaginary unit,  $k$  is the wavenumber, and the quantity  $q_L$  is related to sound pressure  $p_L$  as in equation (1) with subscript "i" replaced by "L". The quantity  $p_+$  in Figure 2 denotes the total sound pressure downstream, and the quantity  $p_-$  the sound pressure upstream, caused by the actuator elements.

Two delays are further introduced. The delay  $\tau_L$  is the time the sound needs to propagate from the detector position to the middle of the actuator system

$$\tau_L = \frac{L}{c_0} . \quad (3)$$

The delay  $\tau$  corresponds to the acoustic delay between the outermost monopoles

$$\tau = \frac{d}{c_0} . \quad (4)$$

## 2.2 Basic two-element construction

The basic two-element construction to be examined here consists of two actuator elements of monopole type located at  $x = \pm d/2$  thus having a mutual distance of  $d$  as depicted in Figure 3. The corresponding field and source quantities are presented in Figure 4. The actuator elements produce volume velocities  $q_1$  and  $q_2$ .

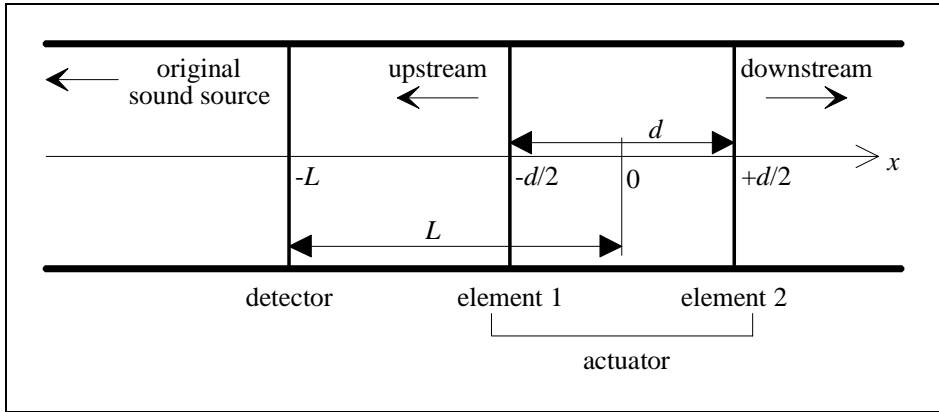


Figure 3. Schematic presentation of the geometry of the two-element actuator construction in a duct.

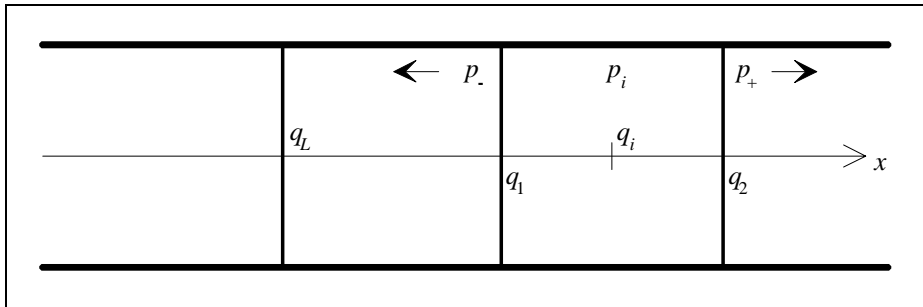


Figure 4. Schematic presentation of the field and source quantities in the two-element actuator construction in a duct.

### 3. Well-known unidirectional solutions

This section describes the unidirectional actuator systems that have been introduced in literature previously and that are somehow related to the JMC method. The three-element solutions of Swinbanks [15], Berengier and Roure [17], and La Fontaine and Shepherd [18] are based on quite a different principle than the JMC method. Also, they cannot be taken as any special solutions of the JMC element, so they are not presented here.

#### 3.1 Three-element solution according to the JMC method

The control system feeding the actuators forming the monopole and dipole is illustrated in Figure 5. In the works of Jessel, Mangiante, and Canévet [30, 32] the dipole weighting  $a$  and monopole weighting  $b$  are realized by phase shifts and magnitude equalization, tuned experimentally. No pertinent mathematical expressions for them are given. The case in which  $a = b = 1$  corresponds the basic solution without modifications.

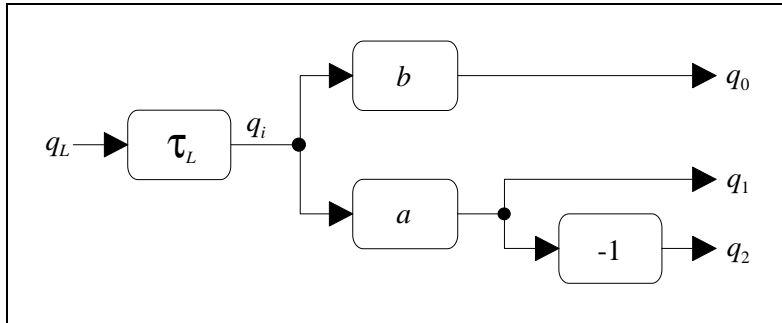


Figure 5. Control system of a modified three-element JMC actuator.

#### 3.2 Two-element solutions

Swinbanks' solution and the two-element maximally efficient source of Winkler and Elliott are presented. The former is an ideal unidirectional solution, giving the same volume velocities as the new ideal sources of this report, but having a

different way of realization. The latter is a suboptimal solution that can be defined also by the general presentation of the new source types of this report.

### 3.2.1 Swinbanks' solution

A two-element actuator works ideally unidirectionally, if the phases of the upstream radiation components of the actuator elements are opposite and the magnitudes are equal. The actuator system, developed by Swinbanks [15, 16], realizes this idea by delaying the output  $q_1$  in respect to the output  $q_2$  by the acoustic propagation delay  $\tau$  between the actuators, and by having opposite phases with the volume velocities  $q_1$  and  $q_2$ . The procedure of achieving the unidirectionality leads to the need of magnitude equalization, in order to obtain ideal sound cancellation downstream.

Swinbanks' source has the volume velocities (with delay and equalization taken into account)

$$\begin{aligned} q_1 &= + \frac{q_i e^{-jkd/2}}{2 j \sin(kd)} , \quad x = -\frac{d}{2} \\ q_2 &= - \frac{q_i e^{+jkd/2}}{2 j \sin(kd)} , \quad x = +\frac{d}{2} . \end{aligned} \quad (5)$$

The amplitudes in proportion to  $q_i$  in equation (5) can be expressed as

$$\frac{1}{2 j \sin(kd)} = \frac{1}{2} \frac{c_0 / d}{j \omega} \frac{kd}{\sin(kd)} , \quad (6)$$

where  $\omega$  is the angular frequency. According to equations (5) and (6) the control system of Swinbanks' source can be presented as in Figure 6.

The amplitude factor  $A$  in the control system is according to equation (6)

$$A = \frac{kd}{\sin(kd)} . \quad (7)$$

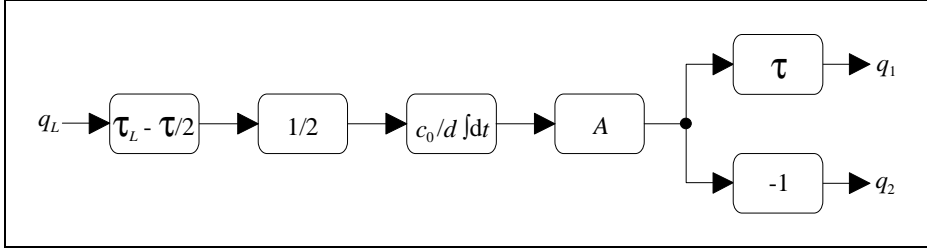


Figure 6. Control system for Swinbanks' two-element actuator with an integrator.

The delay  $\tau/2$  has been subtracted from the propagating delay  $\tau_L$ , to avoid negative delays in the control system.

Swinbanks does not separate the integrator and amplitude factor  $A$ , but rather uses them together, as in equation (6). The separation is done here to compare in an easier way the solution with the new ones, presented in this report with a separate integrator.

The weighting (amplitude factor  $A$  in decibels) is presented in Figure 7. The symbol  $\lambda$  denotes the wavelength of sound. The weighting is singular at frequencies corresponding to the distance  $d$  being a multiple of half the wavelength. Without the separate integrator the weighting would be singular also at zero frequency.

The term  $1/2j\sin(kd)$  (or the integrator and the amplitude factor  $A$  with the constant  $1/2$ ) can be expressed as

$$\frac{1}{2j\sin(kd)} = \frac{e^{-jkd}}{1 - e^{-j2kd}} \quad (8)$$

As shown by Berengier and Roure [17], this suggests that that term can be realized with a positive feedback loop with a delay. This realization is presented in Figure 8.

The Swinbanks' source is ideal, i.e., in theory, the sound cancellation downstream is complete and there is no sound radiation upstream.

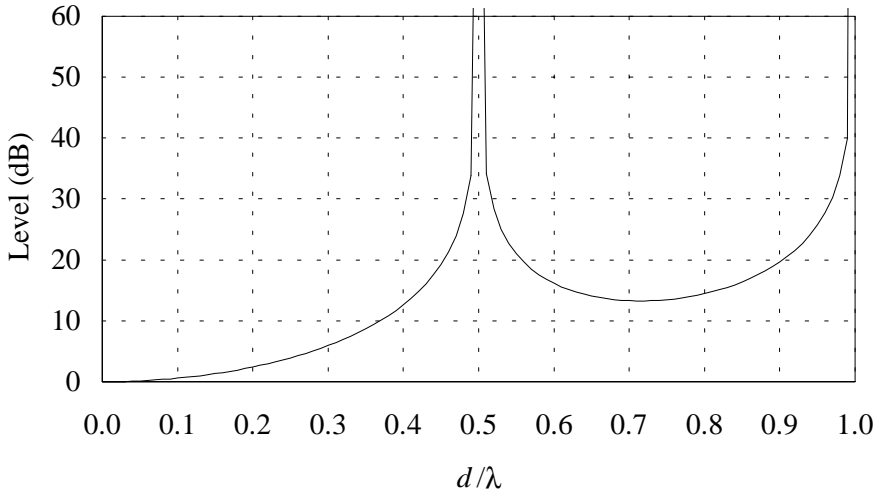


Figure 7. Weighting of Swinbanks' two-element source with a separate integrator.

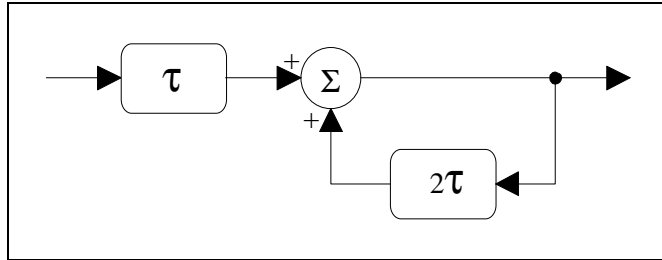


Figure 8. Realization of the integrator and amplitude factor  $A$  for Swinbanks' two-element actuator with a feedback loop with a delay.

### 3.2.2 Maximally efficient source

Winkler and Elliott [14] use the acoustic propagation delay between the two actuators applied to the second actuator, and feed the actuators otherwise in the same phase. This solution is called the "maximally efficient source". It refers to a source eliminating the total sound pressure downstream with least "effort" [3]. The least effort signifies minimizing the square of the absolute values of the volume velocities of the source complex.

The volume velocities of the two-element maximally efficient source of Winkler and Elliott has the volume velocities

$$\begin{aligned} q_1 &= -\frac{q_i}{2} e^{-jkd/2}, \quad x = -\frac{d}{2} \\ q_2 &= -\frac{q_i}{2} e^{+jkd/2}, \quad x = +\frac{d}{2}. \end{aligned} \quad (9)$$

The control system of the maximally efficient source can be presented as in Figure 9.

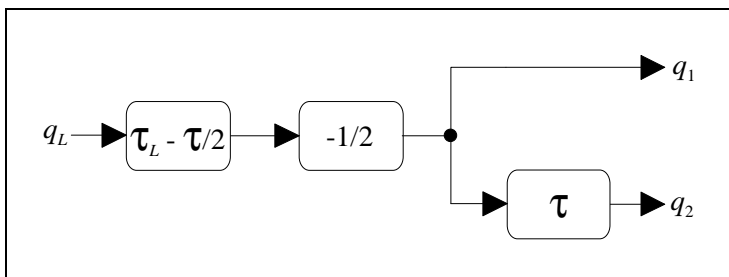
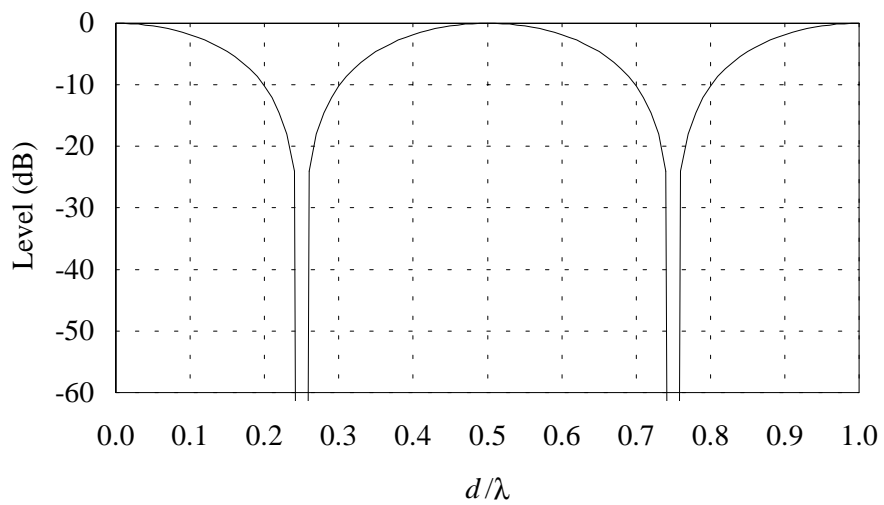


Figure 9. Control system of the maximally efficient source of Winkler and Elliott.

The sound cancellation downstream is complete for the maximally efficient source. However, the actuator is not unidirectional at low frequencies and at frequencies where  $d$  is a multiple of half of the wavelength ( $\lambda/2$ ). The residual sound pressure upstream is presented in Figure 10.



*Figure 10. Residual sound pressure upstream of the maximally efficient source of Winkler and Elliott.*

## 4. New solutions based on the JMC method

In the following, new JMC-based unidirectional structures constructed of three or two actuator elements are derived.

### 4.1 New three-element solutions

#### 4.1.1 Basic solution

The volume velocity produced by the monopole is

$$q_0 = -\frac{q_i}{2}, \quad (10)$$

and those produced by the elements of the dipole are

$$\begin{aligned} q_1 &= +\frac{q_i}{j2kd}, \quad x = -\frac{d}{2} \\ q_2 &= -\frac{q_i}{j2kd}, \quad x = +\frac{d}{2}. \end{aligned} \quad (11)$$

At low frequencies ( $\lambda \gg d$ , where  $\lambda$  is the wavelength) the total sound pressure vanishes downstream and the actuator does not radiate any sound upstream, see Appendix A. At higher frequencies the actuator configuration does not work ideally, due to the approximated realization of the dipole part.

#### 4.1.2 Modified solution

Both the monopole and dipole can be modified by weighting (as a function of frequency), in order to compensate the approximate character of the actuator. Let us denote the weighting of the dipole by  $a$  and that of the monopole by  $b$ . The volume velocity, produced by the monopole, is in this case

$$q_0 = -\frac{bq_i}{2}, \quad (12)$$

and the volume velocities of the monopoles, forming the dipole approximation, are

$$\begin{aligned} q_1 &= +\frac{aq_i}{j2kd}, \quad x = -\frac{d}{2} \\ q_2 &= -\frac{aq_i}{j2kd}, \quad x = +\frac{d}{2}. \end{aligned} \quad (13)$$

The term  $1/jkd$  in the control system can be realized by an integrator. In that case the control system is as in Figure 11. The separate phase shift of  $90^\circ$  is not needed.

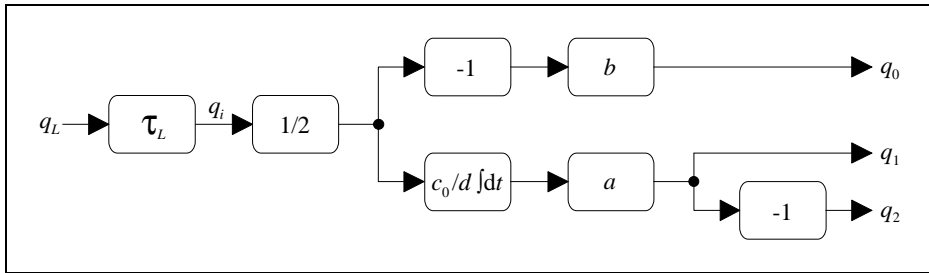


Figure 11. Control system of a modified three-element JMC actuator with an integrator in the dipole control.

The idea of the new solutions is to find optimal and suboptimal mathematical formulae for the weightings  $a$  and  $b$ , the criteria being unidirectionality and sound canceling ability.

#### 4.1.3 Ideal Source and four approximations

The new three-element solutions according to equations (12) and (13) have been given identifications *Ideal Source* and *Approximations 1 – 4*. The explanations for the different solutions are given in Table 1.

The basic solution ( $a = b = 1$ ) is called here Approximation 1. The only new idea in Approximation 1 is the use of the integrator in the control system, to avoid the separate  $90^\circ$  phase shift in the dipole control. Of course, the integrator is present also in the other solutions.

Table 1. Different solutions for the three-element actuators.

Solution	Illustration of solution
Ideal Source	New ideal source, monopole part not modified
Appr. 1	Basic 3-element actuator, neither $a$ nor $b$ optimized
Appr. 2	Maximally efficient source, total sound downstream vanishes
Appr. 3	Dipole part not modified, no upstream radiation
Appr. 4	Dipole part not modified, total sound downstream vanishes

The idea for Approximation 2 is to be a three-element version of the two-element maximally efficient source defined by Winkler and Elliott [14]. Winkler and Elliott have presented only one type of two-element maximally efficient source, so this three-element version is a new one. This solution is not unidirectional at low frequencies, but it has been taken here for the sake of comparison.

Approximations 3 and 4 are solutions where the dipole part is not modified ( $a = 1$ ) and the monopole part is modified by eliminating totally either the upstream or the downstream sound.

Because the basic approximation in the basic solution lies in the dipole part, proper modification of only the dipole part (in which case  $b = 1$ ) leads to the ideal solution.

#### 4.1.4 Weighting functions

The values of the weighting functions can be derived as presented in Appendix A. Also in Appendix A are presented the general relationships for the weighting functions for three special cases: the radiation upstream will not exceed a limiting value, the total sound downstream will not exceed a limiting value, and the case where there is a requirement for the ratio of the upstream and downstream sound pressures.

Table 2 contains the values of  $a$  and  $b$  in different solutions. It should be noted that without the integrator in the control system, the dipole weighting of three-element Ideal Source would be singular at zero frequency.

Table 2. Weighting functions for the three-element solutions.

Solution	$a$	$b$
Ideal	$\frac{kd/2}{\sin(kd/2)}$	1
Appr. 1	1	1
Appr. 2	$\frac{2kd \sin(kd/2)}{1 + 2 \sin^2(kd/2)}$	$\frac{2}{1 + 2 \sin^2(kd/2)}$
Appr. 3	1	$\frac{\sin(kd/2)}{kd/2}$
Appr. 4	1	$2 - \frac{\sin(kd/2)}{kd/2}$

#### 4.1.5 Delay realization of the weightings

As with Swinbanks' source [15] and with the solutions of Berengier and Roure [17], the weightings can be realized with delays and constant magnitude weightings. As an example, consider the dipole weighting of the three-element Ideal Source. It can be easily observed that

$$\frac{c_0}{j\omega d} \frac{kd/2}{\sin(kd/2)} = \frac{e^{-jkd/2}}{1 - e^{-jkd}} \quad (14)$$

Thus the integrator and dipole weighting  $a$  for three-element Ideal Source can be realized as depicted in Figure 12.

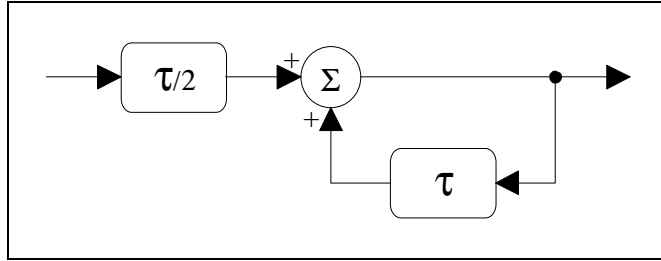


Figure 12. Realization of the integrator and dipole weighting by delays for three-element Ideal Source.

The weightings for Approximations 1 – 4 can be realized similarly with delays and constant weightings. However, the short delays require a large amount of digital signal processing power. Moreover, the delay realizations in the approximations are quite complicated. For these reasons they are not handled in this report.

#### 4.1.6 Residual sound pressures

In Table 3 the residual sound pressures for the different solutions are presented.

## 4.2 New two-element solutions

In the three-element approximation of the JMC element the ideal dipole part of the actuator is approximated by two monopoles in opposite phases, and the monopole part is realized by one monopole between the dipole components. In this section we show how this three-element JMC element can be realized by two elements only.

In two-element approximations of the JMC element a phase shift of  $180^\circ$  between the volume velocities of the elements ensures that the two elements radiate approximately the dipole part of the ideal JMC source. Besides that, also the volume velocity produced by the ideal monopole is approximately included in the elements. Consequently, the total volume velocities  $q_1$  and  $q_2$  of the elements, see Figure 4, are combinations of the volume velocities of the approximated monopole and dipole parts of radiation. The approximations of the system can be compensated by proper weightings as a function of frequency.

Table 3. Residual sound pressures down- and upstream for the three-element solutions.

Solution	$\frac{p_+}{p_i e^{-jkx}}$	$\frac{p_-}{p_i e^{+jkx}}$
Ideal	–	–
Appr. 1	$\frac{1}{2} \left( 1 - \frac{\sin(kd/2)}{kd/2} \right)$	$\frac{1}{2} \left( \frac{\sin(kd/2)}{kd/2} - 1 \right)$
Appr. 2	–	$-\frac{1 - 2 \sin^2(kd/2)}{1 + 2 \sin^2(kd/2)}$
Appr. 3	$1 - \frac{\sin(kd/2)}{kd/2}$	–
Appr. 4	–	$\frac{\sin(kd/2)}{kd/2} - 1$

#### 4.2.1 Basic solution

The inter-channel delay, corresponding to the acoustic propagation delay between the actuator elements, can be selected in the monopole part of the volume velocity  $q_1$  in respect to that of the volume velocity  $q_2$  to ensure that the monopole part of the radiation is correct downstream. This ensures that the residual sound pressure downstream is minimized. This kind of selection of the delay leads to a solution where the residual sound pressure downstream is smaller and upstream higher. In that case the volume velocities are

$$\begin{aligned}
 q_1 &= +\frac{1}{2} \left( \frac{1}{jkd} - \frac{1}{2} e^{+jkd/2} \right) q_i, \quad x = -\frac{d}{2} \\
 q_2 &= -\frac{1}{2} \left( \frac{1}{jkd} + \frac{1}{2} e^{-jkd/2} \right) q_i, \quad x = +\frac{d}{2}.
 \end{aligned} \tag{15}$$

In the expressions for the volume velocities of the radiators, the first parts are related to the dipole radiation and the second parts to the monopole radiation.

The inter-channel delay can be selected also to ensure that the monopole part of the radiation is correct upstream. This kind of selection of the delay leads to a solution where the residual sound pressure upstream is smaller and downstream higher. In that case the volume velocities are

$$\begin{aligned} q_1 &= +\frac{1}{2}\left(\frac{1}{jkd} - \frac{1}{2}e^{-jkd/2}\right)q_i, \quad x = -\frac{d}{2} \\ q_2 &= -\frac{1}{2}\left(\frac{1}{jkd} + \frac{1}{2}e^{+jkd/2}\right)q_i, \quad x = +\frac{d}{2}. \end{aligned} \quad (16)$$

One more selection is the one where there are *no delays* in the monopole parts ( $\tau = 0$ ). This kind of selection leads to a solution where the error is distributed to the residual sound pressure up- and downstream. The volume velocities are in this case

$$\begin{aligned} q_1 &= +\frac{1}{2}\left(\frac{1}{jkd} - \frac{1}{2}\right)q_i, \quad x = -\frac{d}{2} \\ q_2 &= -\frac{1}{2}\left(\frac{1}{jkd} + \frac{1}{2}\right)q_i, \quad x = +\frac{d}{2}. \end{aligned} \quad (17)$$

With all the selected delays, at low frequencies the total sound pressure downstream vanishes and the actuator does not radiate sound upstream, see Appendix B. However, at higher frequencies the actuator configuration does not work ideally, due to the approximated realizations of the monopole and dipole.

#### 4.2.2 Modified solution with three choices of inter-channel delay optimization

As with the three-element solutions, also in the approximation combined of two elements both the monopole and dipole parts can be modified by a weighting (as a function of frequency), in order to compensate the approximate character of the monopole and dipole radiation. Let us denote the dipole weighting as  $a$  and

the monopole weighting as  $b$ , as with the three-element solutions. If the inter-channel delay is optimized downstream, the volume velocities are

$$\begin{aligned} q_1 &= +\frac{1}{2}\left(\frac{a}{jkd} - \frac{b}{2}e^{+jkd/2}\right)q_i, \quad x = -\frac{d}{2} \\ q_2 &= -\frac{1}{2}\left(\frac{a}{jkd} + \frac{b}{2}e^{-jkd/2}\right)q_i, \quad x = +\frac{d}{2}. \end{aligned} \quad (18)$$

The control system, feeding the actuators, is as shown in Figure 13. The case in which  $a = b = 1$  corresponds the basic solution without any modifications.

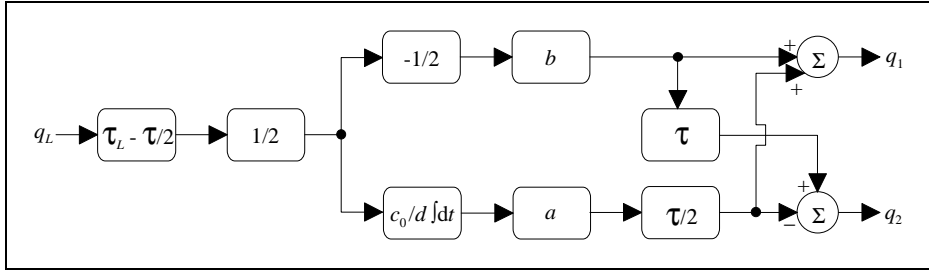


Figure 13. Control system of a two-element actuator with the inter-channel delay optimized downstream.

If the inter-channel delay is optimized upstream, the volume velocities are

$$\begin{aligned} q_1 &= +\frac{1}{2}\left(\frac{a}{jkd} - \frac{b}{2}e^{-jkd/2}\right)q_i, \quad x = -\frac{d}{2} \\ q_2 &= -\frac{1}{2}\left(\frac{a}{jkd} + \frac{b}{2}e^{+jkd/2}\right)q_i, \quad x = +\frac{d}{2}. \end{aligned} \quad (19)$$

In this case the control system, feeding the actuators, is shown in Figure 14.

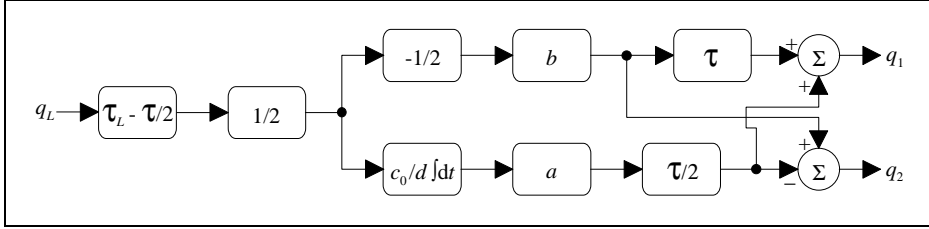


Figure 14. Control system of a two-element actuator with the inter-channel delay optimized upstream.

If there is no inter-channel delay, the volume velocities are

$$\begin{aligned}
 q_1 &= +\frac{1}{2} \left( \frac{a}{jkd} - \frac{b}{2} \right) q_i, \quad x = -\frac{d}{2} \\
 q_2 &= -\frac{1}{2} \left( \frac{a}{jkd} + \frac{b}{2} \right) q_i, \quad x = +\frac{d}{2}.
 \end{aligned}
 \tag{20}$$

In this case the control system feeding the actuators is presented in Figure 15.

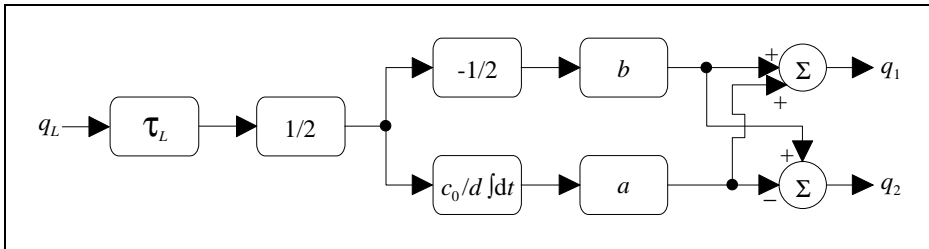


Figure 15. Control system of a two-element actuator with no inter-channel delay.

### 4.2.3 Ideal Source and six approximations

The two-element solutions according to equations (18), (19), and (20) have been given identifications *Ideal Source* and *Approximations 5 – 10*. The explanations for the different solutions are given in Table 4. All of the solutions in Table 1 can be realized with any of the three possibilities of the inter-channel delay.

Table 4. Different solutions for the two-element actuators.

Solution	Illustration of solution
Ideal Source	Monopole and dipole parts modified, no upstream radiation, total sound downstream vanishes
Appr. 5	Basic two-element solution, neither $a$ nor $b$ optimized
Appr. 6	Maximally efficient source, total sound downstream vanishes
Appr. 7	Monopole part not modified, no upstream radiation
Appr. 8	Monopole part not modified, total sound downstream vanishes
Appr. 9	Dipole part not modified, no upstream radiation
Appr. 10	Dipole part not modified, total sound downstream vanishes

Approximation 6 with the inter-channel delay optimized downstream is the same as the maximally efficient source of Winkler and Elliott [14] of equation (9), so it is not a new solution. However, Approximation 6 with the inter-channel delay optimized upstream and with no inter-channel delay are new solutions. They are also called maximally efficient sources (but not devoted to Winkler and Elliott) because the logic for selecting their weightings is the same as that of the maximally efficient source of Winkler and Elliott, see Appendix B.

#### 4.2.4 Weighting functions

The values of the weighting functions can be derived as shown in Appendix B. Also in Appendix B are presented the general relationships for the weighting functions for three special cases: the radiation upstream will not exceed a limiting value, the total sound downstream will not exceed a limiting value, and the

case where there is a requirement for the ratio of the upstream and downstream sound pressures.

Table 5, Table 6, and Table 7 contain the values of  $a$  and  $b$  in different solutions for the different inter-channel delays.

*Table 5. Weighting functions for the two-element solutions with the inter-channel delay optimized downstream.*

Solution	$a$	$b$
Ideal	$\frac{\cos(kd)}{\cos^2(kd/2)} \frac{kd/2}{\sin(kd/2)}$	$\frac{1}{\cos^2(kd/2)}$
Appr. 5	1	1
Appr. 6	0	2
Appr. 7	$\cos(kd) \frac{(kd/2)}{\sin(kd/2)}$	1
Appr. 8	$\frac{kd/2}{\sin(kd/2)}$	1
Appr. 9	1	$\frac{1}{\cos(kd)} \frac{\sin(kd/2)}{(kd/2)}$
Appr. 10	1	$2 - \frac{\sin(kd/2)}{kd/2}$

#### 4.2.5 Delay realization of the weightings

As with Swinbanks' source [15] and with the solutions of Berengier and Roure [17], the weightings can be realized by delays and constant magnitude weightings. As an example, consider dipole weighting of two-element Ideal Source with no inter-channel delay. It can be easily observed that

Table 6. Weighting functions for the two-element solutions with the inter-channel delay optimized upstream.

Solution	$a$	$b$
Ideal	$\frac{1}{\cos^2(kd/2)} \frac{kd/2}{\sin(kd/2)}$	$\frac{1}{\cos^2(kd/2)}$
Appr. 5	1	1
Appr. 6	$2kd \sin(kd/2)$	2
Appr. 7	$\frac{kd/2}{\sin(kd/2)}$	1
Appr. 8	$(2 - \cos(kd)) \frac{kd/2}{\sin(kd/2)}$	1
Appr. 9	1	$\frac{\sin(kd/2)}{kd/2}$
Appr. 10	1	$\frac{1}{\cos(kd)} \left( 2 - \frac{\sin(kd/2)}{kd/2} \right)$

$$\begin{aligned}
 \frac{c_0}{j\omega d} \frac{kd/2}{\sin(kd/2)} &= \frac{e^{-jkd/2}}{1 - e^{-jkd}} \\
 \frac{1}{2 \cos(kd/2)} &= \frac{e^{-jkd/2}}{1 + e^{-jkd}} \quad .
 \end{aligned} \tag{21}$$

So the integrator and dipole weighting  $a$  for two-element Ideal Source without inter-channel delay can be realized as presented in Figure 16. This is just the same as with three-element Ideal Source (see Figure 12).

Table 7. Weighting functions for the two-element solutions with no inter-channel delay.

Solution	$a$	$b$
Ideal	$\frac{kd/2}{\sin(kd/2)}$	$\frac{1}{\cos(kd/2)}$
Appr. 5	1	1
Appr. 6	$kd \sin(kd/2)$	$2 \cos(kd/2)$
Appr. 7	$\cos(kd/2) \frac{kd/2}{\sin(kd/2)}$	1
Appr. 8	$(2 - \cos(kd/2)) \frac{kd/2}{\sin(kd/2)}$	1
Appr. 9	1	$\frac{1}{\cos(kd/2)} \frac{\sin(kd/2)}{kd/2}$
Appr. 10	1	$\frac{1}{\cos(kd/2)} \left( 2 - \frac{\sin(kd/2)}{kd/2} \right)$

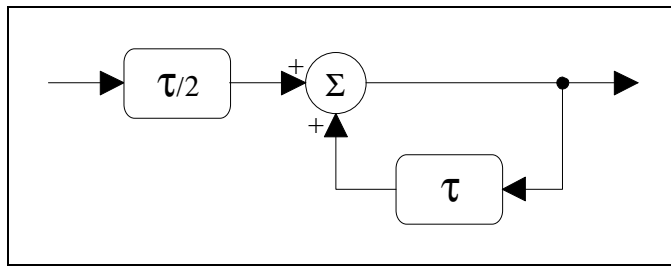
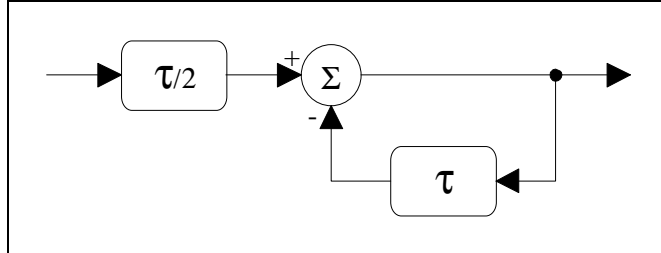


Figure 16. Realization of the integrator and dipole weighting by delays for two-element Ideal Source with no inter-channel delay.

Also the monopole weighting  $b$  (with the constant  $\frac{1}{2}$ ) for two-element Ideal Source without inter-channel delay can be realized using a delay loop as depicted in Figure 17.



*Figure 17. Realization of monopole weighting by delays for two-element Ideal Source with no inter-channel delay.*

The weightings for two-element Ideal Source with other inter-channel delays, and also the weightings for Approximations 5–10 can be realized similarly with delays and constant weightings. However, the short delays require a lot of signal processing power, so these solutions are not very attractive. Moreover, the other delay realizations are much more complicated than presented here. For these reasons they are not handled in this report. Also concerning the Ideal Sources, the outputs of all of them are equal despite the choice of the inter-channel delay. It is not worthwhile to present the delay realizations for other Ideal Sources giving the same output as presented here, but with much more complicated systems.

#### 4.2.6 Residual sound pressures

In Table 8, Table 9, and Table 10 the residual sound pressures for the different solutions for the different inter-channel delays are presented.

Table 8. Residual sound pressures down- and upstream for the two-element solutions with the inter-channel delay optimized downstream.

Solution	$\frac{P_+}{p_i e^{-jkx}}$	$\frac{P_-}{p_i e^{+jkx}}$
Ideal	–	–
Appr. 5	$\frac{1}{2} \left( 1 - \frac{\sin(kd/2)}{kd/2} \right)$	$\frac{1}{2} \left( \frac{\sin(kd/2)}{kd/2} - \cos(kd) \right)$
Appr. 6	–	$-\cos(kd)$
Appr. 7	$\sin^2(kd/2)$	–
Appr. 8	–	$\sin^2(kd/2)$
Appr. 9	$1 - \frac{\cos^2(kd/2) \sin(kd/2)}{\cos(kd) (kd/2)}$	–
Appr. 10	–	$1 - \cos^2(kd/2) \left( 2 - \frac{\sin(kd/2)}{kd/2} \right)$

Table 9. Residual sound pressures down- and upstream for the two-element solutions with the inter-channel delay optimized upstream.

Solution	$\frac{P_+}{p_i e^{-jkx}}$	$\frac{P_-}{p_i e^{+jkx}}$
Ideal	–	–
Appr. 5	$\frac{1}{2} \left( 2 - \cos(kd) - \frac{\sin(kd/2)}{kd/2} \right)$	$\frac{1}{2} \left( \frac{\sin(kd/2)}{kd/2} - 1 \right)$
Appr. 6	–	$-\cos(kd)$
Appr. 7	$\sin^2(kd/2)$	–
Appr. 8	–	$\sin^2(kd/2)$
Appr. 9	$1 - \cos^2(kd/2) \frac{\sin(kd/2)}{kd/2}$	–
Appr. 10	–	$\frac{1}{\cos(kd)} \left( -1 + \cos^2(kd/2) \frac{\sin(kd/2)}{kd/2} \right)$

Table 10. Residual sound pressures down- and upstream for the two-element solutions with no inter-channel delay.

Solution	$\frac{P_+}{P_i e^{-jkx}}$	$\frac{P_-}{P_i e^{+jkx}}$
Id. 3	–	–
Appr. 5	$\frac{1}{2} \left( 2 - \cos(kd/2) - \frac{\sin(kd/2)}{kd/2} \right)$	$\frac{1}{2} \left( \frac{\sin(kd/2)}{kd/2} - \cos(kd/2) \right)$
Appr. 6	–	$-\cos(kd)$
Appr. 7	$1 - \cos(kd/2)$	–
Appr. 8	–	$1 - \cos(kd/2)$
Appr. 9	$1 - \frac{\sin(kd/2)}{kd/2}$	–
Appr. 10	–	$\frac{\sin(kd/2)}{kd/2} - 1$

## 5. Comparison of the new unidirectional solutions

In this section the three- and two-element unidirectional solutions are compared. Their weighting functions and obtainable attenuation both down- and upstream are considered.

### 5.1 Three-element solutions

#### 5.1.1 Weighting functions

Figure 18 and Figure 19 display the weighting of the three-element solutions in graphical forms.

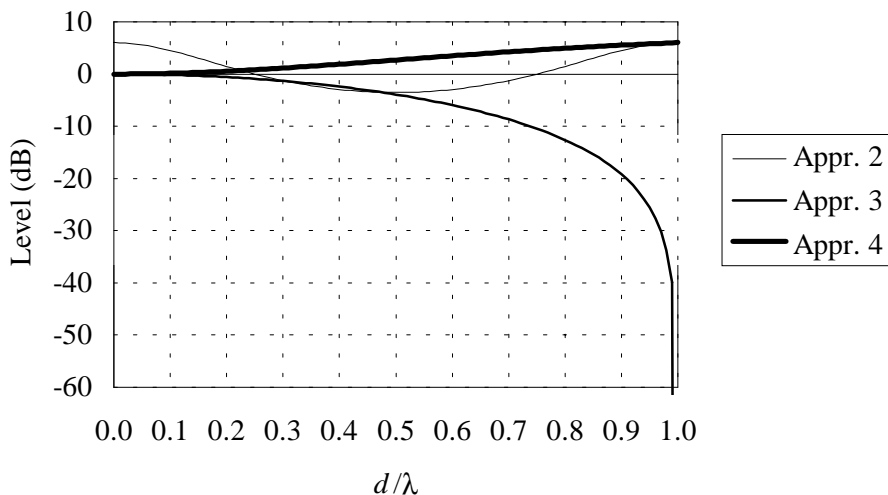


Figure 18. Applied monopole weighting for the three-element solutions.

The continuous available frequency band, due to weighting, is the frequency band from zero frequency to the first frequency where the weighting tends to infinite. In practice, the useful frequency band is narrower than this definition suggests.

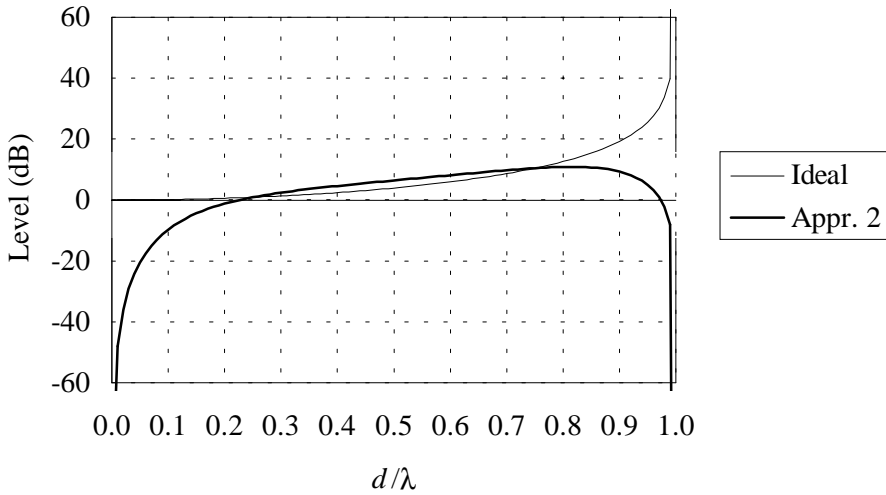


Figure 19. Applied dipole weighting for the three-element solutions.

With three-element Ideal Source the dipole weighting approaches infinity when  $d$  is a multiple of the wavelength, restricting the available frequency band. Approximations 1 – 4 do not have clear restrictions for the available continuous frequency band, due to weightings. Without the integrator in the control system, the weighting of three-element Ideal Source would be singular at zero frequency.

### 5.1.2 Residual sound pressures

Figure 20 and Figure 21 present the residual sound pressure downstream and the sound pressure radiated upstream in proportion to the original sound pressure for the three-element approximations.

Three-element Ideal Source causes the total sound pressure downstream to vanish and does not radiate any sound upstream. Approximations 2 and 4 cause the total sound pressure downstream to vanish, but they generate sound radiation upstream. Approximation 3 does not radiate any sound upstream, but does not totally eliminate the sound downstream. Approximation 1 does not totally eliminate the sound downstream, and generates sound radiation upstream.

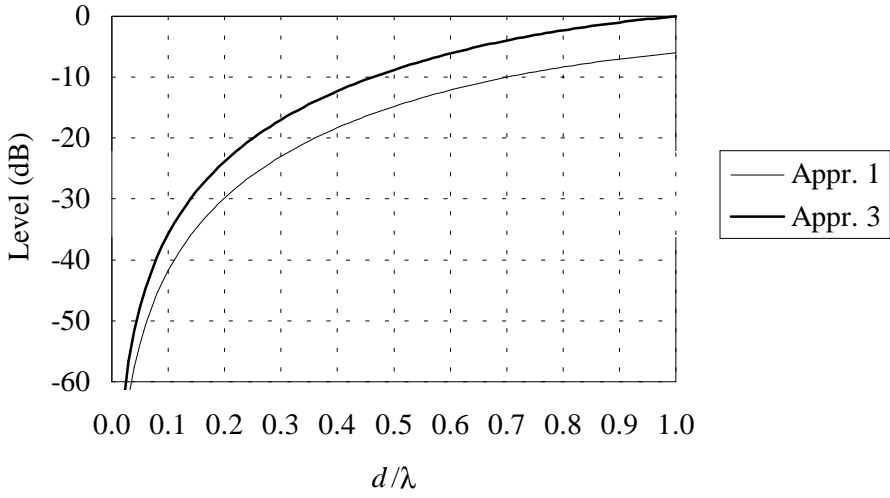


Figure 20. Residual sound pressures of the three-element approximations downstream.

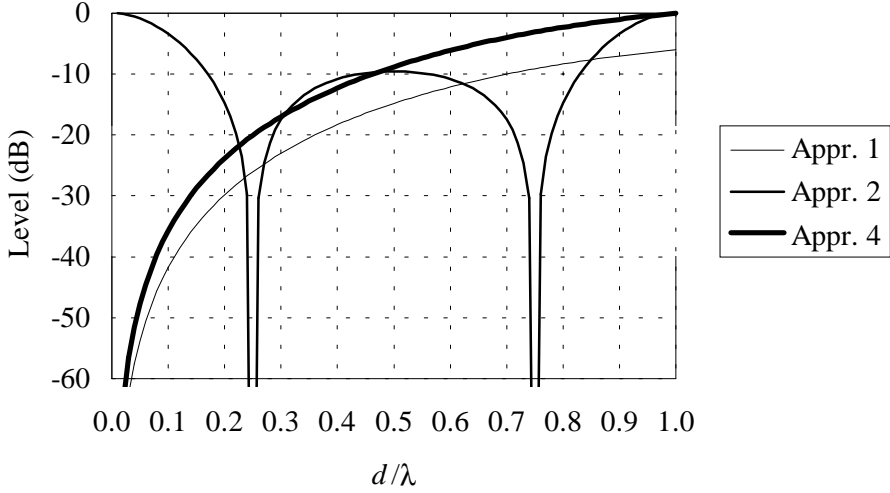


Figure 21. Residual sound pressures of the three-element approximations upstream.

At low frequencies and at frequencies where  $d$  is a multiple of wavelength ( $\lambda$ ), Approximation 2 (maximally efficient source) reflects the sound totally upstream. It is thus not a unidirectional source.

The continuous available frequency band, due to residual sound pressures, is the frequency band from zero frequency to the first frequency above which the magnitude of the residual sound pressure up- or downstream is higher than that of the incoming sound pressure. In practice, the useful frequency band is narrower than this definition suggests.

Three-element Ideal Source is ideal in respect that there are no residual sound pressures up- or downstream. For Approximation 4 the continuous available frequency band is limited by the upstream residual sound pressure, and for Approximation 3 by the downstream residual sound pressure, with an upper frequency limit corresponding a wavelength obeying  $d = \lambda$ . For Approximations 1 and 2 there is no limit for the continuous available frequency band due to residual sound pressures. With Approximation 1 the residual sound pressures approach the defined limit when the frequency approaches infinite.

## 5.2 Two-element solutions

Two-element Ideal Sources cause the total sound pressure downstream to vanish and do not radiate any sound upstream. Approximations 6, 8, and 10 cause the total sound pressure downstream to vanish, but generate sound radiation upstream. Approximations 7 and 9 do not radiate any sound upstream, but do not totally eliminate the sound downstream. Approximation 5 does not totally eliminate the sound downstream, and generates sound radiation upstream. At low frequencies, Approximation 6 (maximally efficient source) reflects the sound totally upstream. Strictly speaking, it is thus not a unidirectional source.

The output volume velocities of all the three variations of two-element Ideal Source are identical with those of Swinbanks' two-element actuator [15], although the procedure of attaining them is quite different. The control system of the Swinbanks' two-element actuator may seem simple in relation to those of two-element Ideal Source. However, the delayless version of two-element Ideal Source has the advantage of no separate phase shift between the volume veloci-

ties of the elements, which turns out to be advantageous in the practical implementation of digital control systems.

### 5.2.1 Weighting functions

The weightings of Approximation 5 are unity in all cases. The weighting functions and the corresponding frequency limits of other structures are discussed in the following sections.

#### 5.2.1.1 Two-element Ideal Source

The weighting function of the dipole part for two-element Ideal Source is presented in Figure 22, and that of the monopole part in Figure 23, for different inter-channel delays. It can be seen that the delay optimization downstream requires the dipole weighting to be zero ( $-\infty$  in dB) at  $d = \lambda/4$  and  $3\lambda/4$ . The delay optimization up- or downstream requires the dipole weighting to be infinite at  $d = \lambda/2$ . In the delayless case there is no such requirement. However, whatever the delay is, the monopole weighting tends to infinite at  $d = \lambda/2$ . Thus, the available continuous frequency band is limited due to weighting to an upper frequency limit corresponding to  $d = \lambda/2$ , independently of the inter-channel delay optimization.

#### 5.2.1.2 Approximation 6

Approximation 6 is the two-element maximally efficient source. The dipole weighting of Approximation 6 for different inter-channel delays is presented in Figure 24 and the monopole weighting of the same approximation in Figure 25. There is no dipole part of radiation (weighting is  $-\infty$  in dB) for the downstream optimized delay. In Figure 24 it can be seen that for other cases there is a non-vanishing dipole part of radiation, except at frequencies corresponding to  $d$  being a multiple of the wavelength. In Figure 25 it can be observed that the delay optimization both up- or downstream leads to a constant monopole weighting. The delayless case leads to a monopole weighting which is a function of frequency having a zero ( $-\infty$  dB) at a frequency corresponding to  $d$  being half of the wavelength (or an odd multiple of it). There are no frequencies with infinite weighting values, so the weightings themselves do not cause any limitations to the continuous available frequency band.

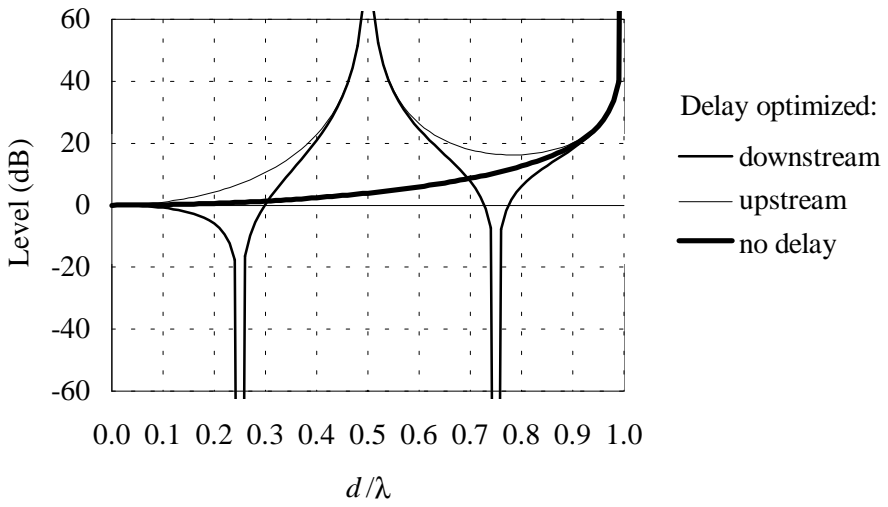


Figure 22. Dipole weighting of two-element Ideal Source for different inter-channel delays.

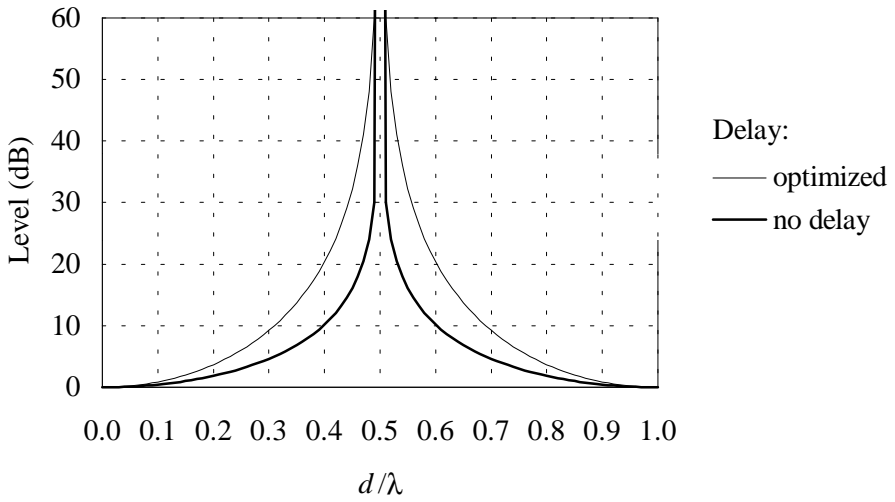


Figure 23. Monopole weighting of two-element Ideal Source for different inter-channel delays.

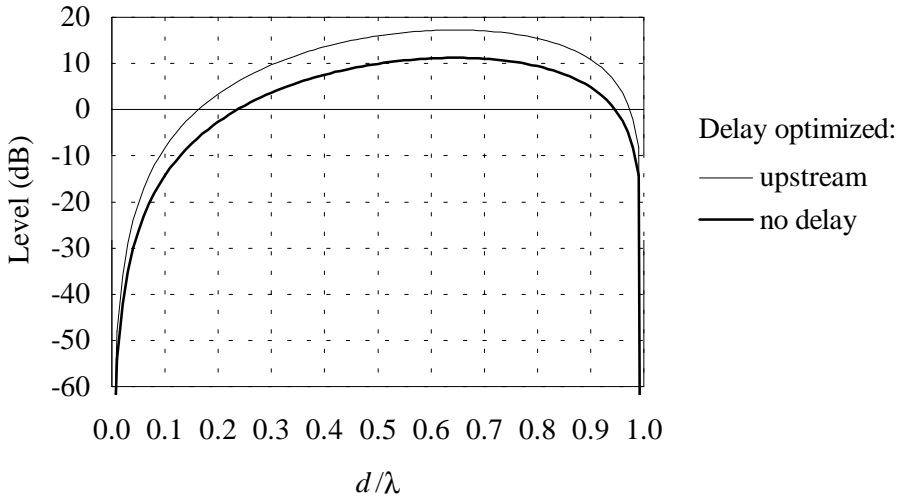


Figure 24. Dipole weighting of Approximation 6 for different inter-channel delays.

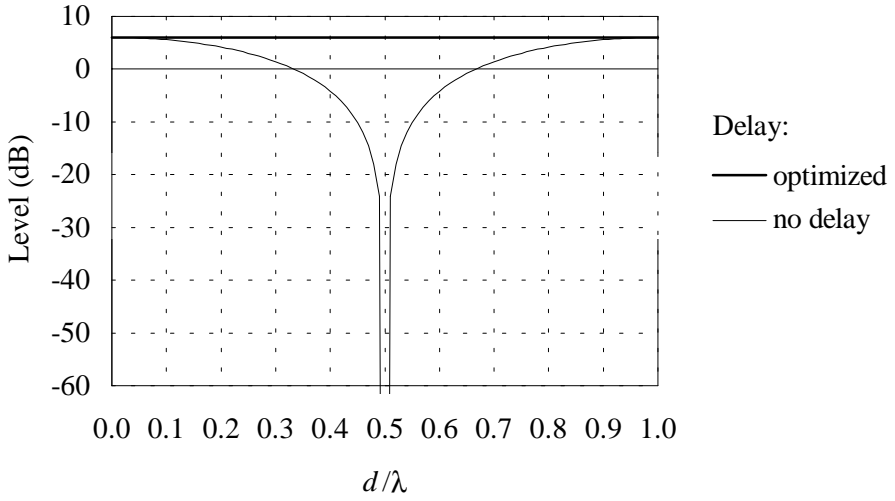


Figure 25. Monopole weighting of Approximation 6 for different inter-channel delays.

### 5.2.1.3 Approximations 7 and 8

The monopole weightings of Approximations 7 and 8 are unity for all cases of delay optimization. The dipole weighting of Approximation 7 for different inter-channel delays is presented in Figure 26. From that figure one can see that the delay optimization downstream for Approximation 7 leads to zeros ( $-\infty$  dB) in the dipole weighting values at the same frequencies as for two-element Ideal Source. In the delayless case, the dipole weighting value is zero ( $-\infty$  dB) at the frequency corresponding to  $d$  being half of the wavelength. Whatever the delay is with Approximation 7, the dipole weighting does not tend to infinite at  $d$  being half of the wavelength, as was the case with two-element Ideal Source for up- and downstream optimized delay. The dipole weighting approaches infinite when  $d$  approaches the wavelength, similarly as with two-element Ideal Source. So the available continuous frequency band, due to weighting, is twice that of two-element Ideal Source, limited to an upper frequency limit corresponding to  $d = \lambda$ , independently of the inter-channel delay optimization.

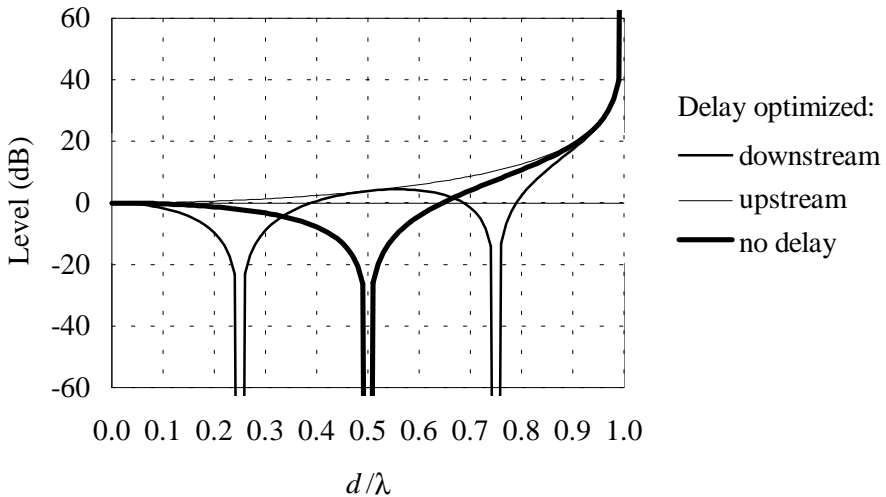


Figure 26. Dipole weighting of Approximation 7 for different inter-channel delays.

The monopole weighting of Approximation 8 is unity in all cases, and the dipole weighting for different inter-channel delays is presented in Figure 27. From that

figure one can see that the dipole weighting for Approximation 8 is quite a smooth function of frequency, except at  $d$  being a multiply of the wavelength where the weighting tends to infinite. The available continuous frequency band, due to weighting, is the same as with Approximation 7, being twice that of two-element Ideal Source.

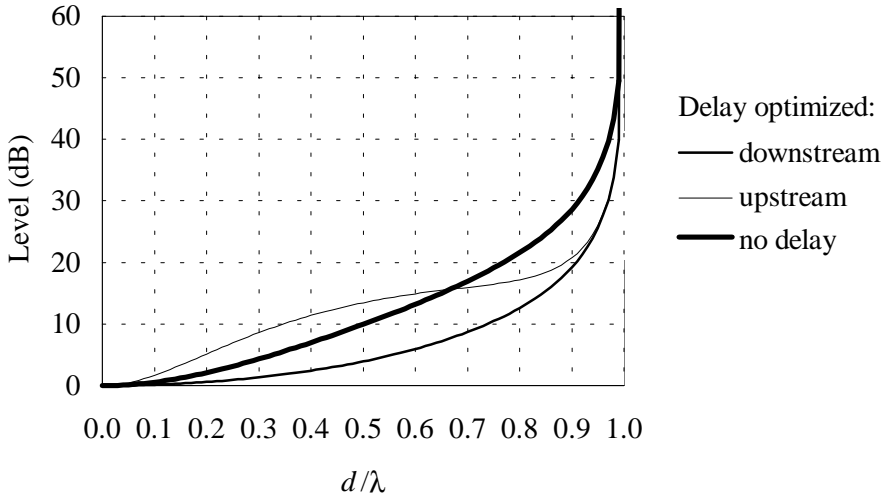


Figure 27. Dipole weighting of Approximation 8 for different inter-channel delays.

#### 5.2.1.4 Approximations 9 and 10

The monopole weighting of Approximation 9 for different inter-channel delays is presented in Figure 28 and that of Approximation 10 in Figure 29. From Figure 28 it can be seen that at  $d$  being a multiple of wavelength, the monopole weighting is zero ( $-\infty$  dB). From the figures it can be seen that the weighting of Approximation 9 for delay optimization downstream and that of Approximation 10 for delay optimization upstream are infinite at  $d = \lambda/4$  and  $3\lambda/4$ . Since the continuous available frequency band due to weighting for those cases is very narrow (half that of two-element Ideal Source), these Approximations are not suitable to be used with those delay optimizations. With the delayless cases the weightings are infinite for both Approximations at  $d$  being half of the wavelength; thus the continuous available frequency band, due to weighting, is the

same as with two-element Ideal Source. The weighting causes no limitations on the frequency band for Approximation 9 with delay optimized upstream and for Approximation 10 with delay optimized downstream.

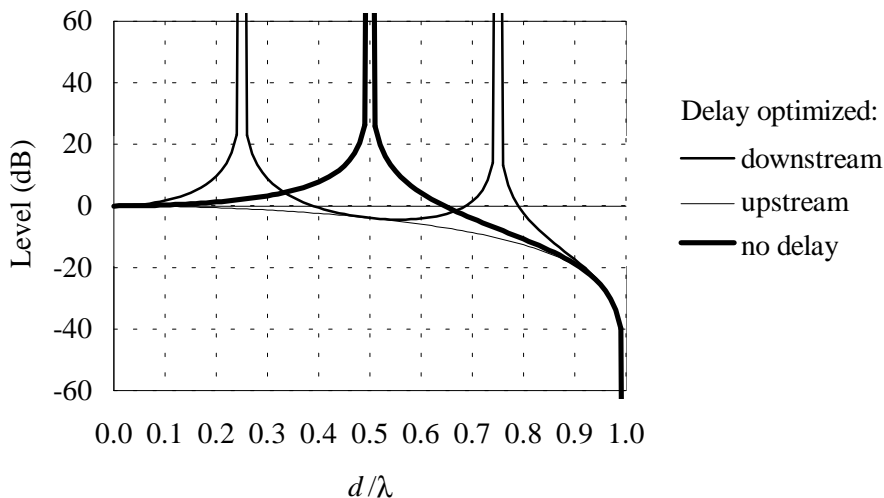


Figure 28. Monopole weighting of Approximation 9 for different inter-channel delays.

### 5.2.2 Residual sound pressures

Two-element Ideal Source is ideal in respect that there are no residual sound pressures up- or downstream, independently of the inter-channel delay optimization. This fact is due to two-element Ideal Source producing the same volume velocity, independently of the inter-channel delay optimization. Approximation 6 (the two-element maximally efficient source) causes no residual sound downstream. Its residual sound pressure upstream is the same, independently of the inter-channel delay optimization, so it is the same as presented in Figure 10. This fact is similarly due to the maximally efficient source producing the same volume velocity, independently of the inter-channel delay optimization. The residual sound pressure never grows higher than the incoming sound pressure. There are no limitations on the continuous available frequency band for two-element Ideal Source and maximally efficient source.

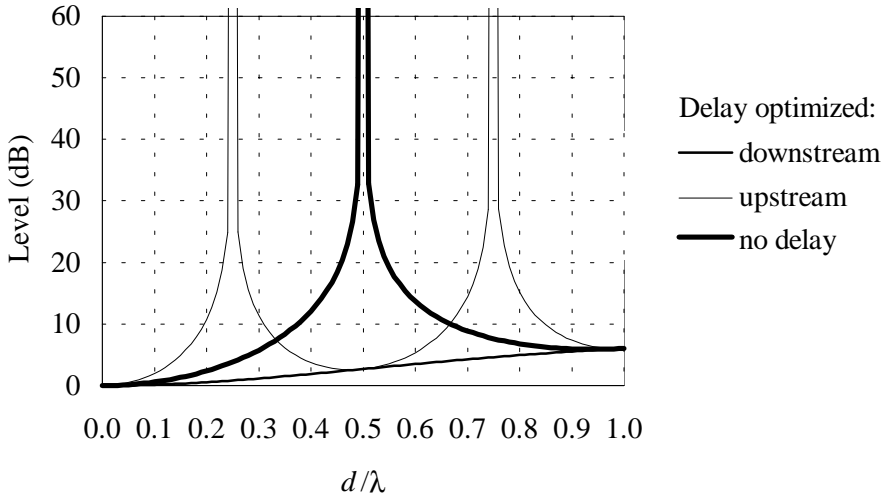


Figure 29. Monopole weighting of Approximation 10 for different inter-channel delays.

### 5.2.2.1 Approximation 5

Approximation 5 denotes the approximation where both of the weighting functions  $a$  and  $b$  are equal to 1, that is, there is no weighting in this basic solution. In Figure 30 the residual sound pressure upstream of Approximation 5 is presented for different inter-channel delays. In Figure 31 the residual sound pressure downstream is presented similarly. It can be seen that below a frequency, corresponding to the wavelength where  $d \approx 0.65 \lambda$ , the delay optimization downstream decreases the residual sound pressure downstream and increases it upstream. If the delay is optimized upstream, the situation is vice versa. Also it can be seen that the sound pressure downstream will be amplified above that frequency if there is no delay optimization. This leads to a continuous available frequency band, due to residual sound pressure, with an upper frequency limit corresponding a wavelength obeying  $d = 0.65 \lambda$ . With the delay optimization upstream, the sound pressure is amplified at lower frequencies leading to a continuous available frequency band, due to residual sound pressure, with an upper frequency limit corresponding a wavelength obeying  $d = 0.39 \lambda$ . This is a very narrow band, so this solution is not recommended.

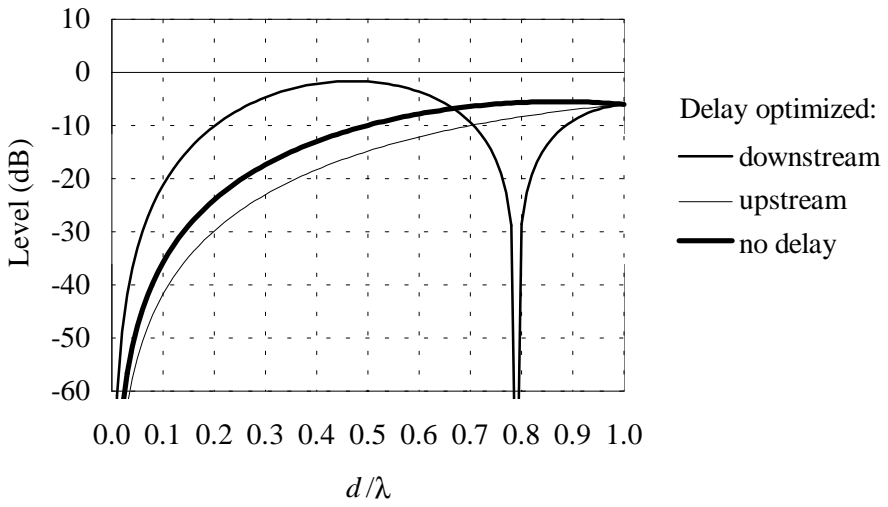


Figure 30. Residual sound pressure upstream of Approximation 5 for different inter-channel delays.

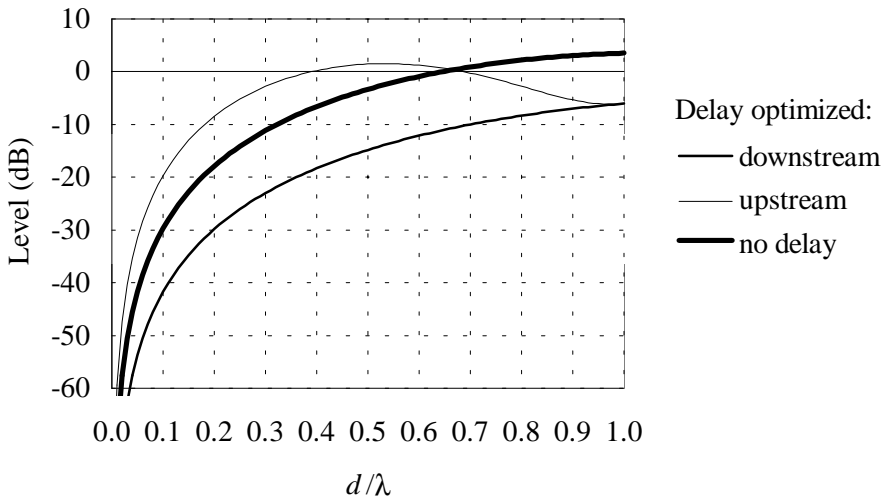


Figure 31. Residual sound pressure downstream of Approximation 5 for different inter-channel delays.

### 5.2.2.2 Approximations 7 and 8

The residual sound pressure downstream of Approximation 7 with and without the inter-channel delay optimization is presented in Figure 32. It can be seen that the capability of the system is independent on the direction of the delay optimization. Also it can be seen that above a frequency, at which  $d = \lambda/2$ , the sound downstream is amplified if no delay optimization is used. So there is a continuous available frequency band, due to residual sound pressure, having the frequency as the upper frequency limit. Below that frequency the residual sound pressure downstream is lower for no delay optimization.

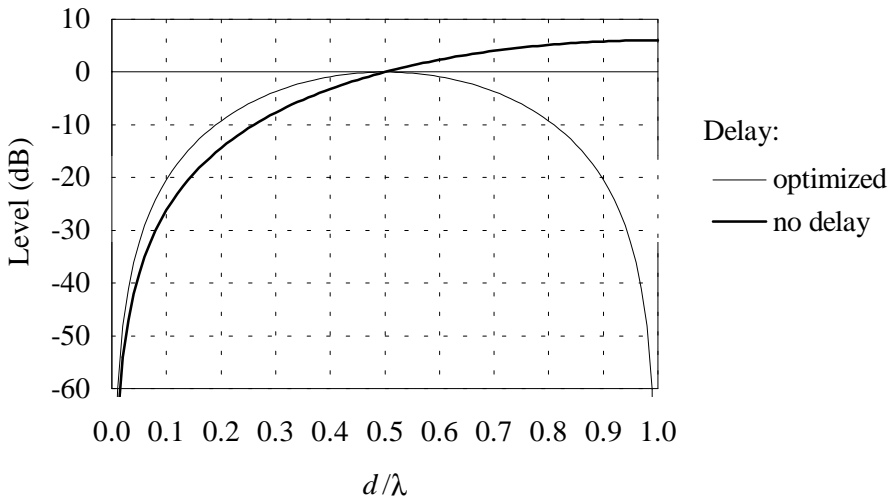


Figure 32. Residual sound pressure downstream of Approximation 7 with and without inter-channel delay optimization.

The residual sound pressure upstream of Approximation 8 is similar to the residual sound pressure downstream of Approximation 7. So the conclusions above can be directly applied to the upstream radiation of Approximation 8.

### 5.2.2.3 Approximations 9 and 10

The residual sound pressure downstream of Approximation 9 for different inter-channel delays is presented in Figure 33. The residual sound pressure upstream

of Approximation 10 is similarly presented in Figure 34. It can be seen that for these approximations there is no reason for using any inter-channel delay optimization. The systems are working better without any inter-channel delays. Especially, the downstream optimization for Approximation 9 and the upstream optimization for Approximation 10 amplify the sound at a very broad frequency band, making those optimizations useless. The continuous available frequency bands, due to residual sound pressure, for those solutions have upper frequency limits corresponding to  $d = 0.2 \lambda$  and  $0.19 \lambda$  respectively. In the case of no inter-channel delays, the residual sound pressure downstream of Approximation 9 is quite the same as the residual sound pressure upstream of Approximation 10. In these cases the continuous available frequency band, due to residual sound pressure, is limited by  $d = \lambda$ .

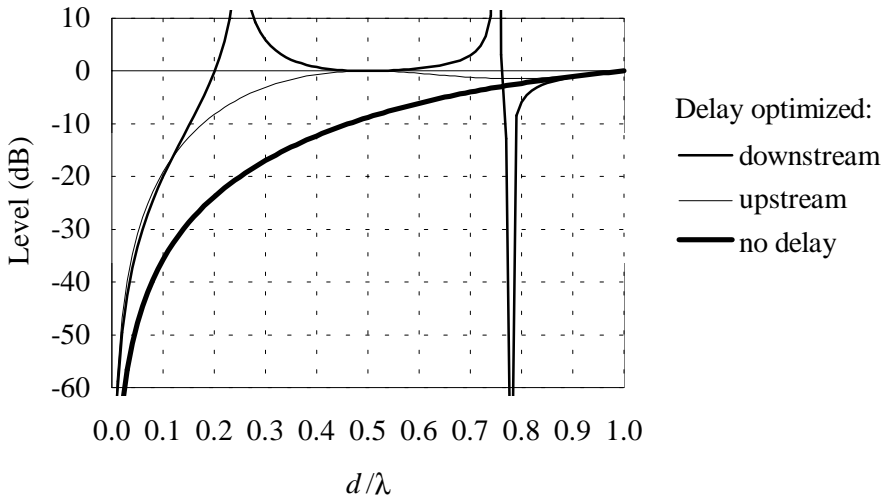


Figure 33. Residual sound pressure downstream of Approximation 9 for different inter-channel delays.

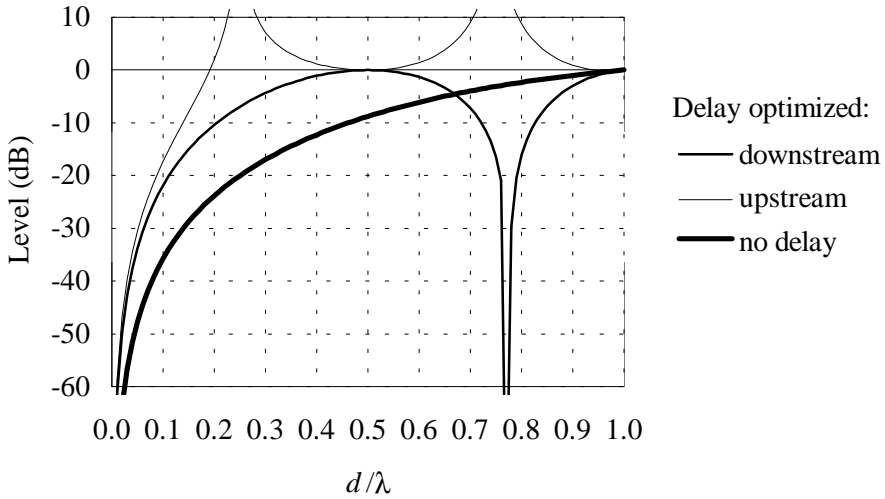


Figure 34. Residual sound pressure upstream of Approximation 10 for different inter-channel delays.

### 5.3 Concluding remarks on the continuous available frequency bands

The limits for continuous available frequency bands due to weightings and due to residual sound pressures are gathered in Table 11 for three-element solutions. The dash (–) indicates that there is no upper limit. The basic solution (Approximation 1) has no frequency limits, although a practical limit would be near  $d = \lambda$ . Approximation 2 has no frequency limits, although at frequencies where  $d = n\lambda$  ( $n = 0, 1, 2, \dots$ ) the residual sound pressures are equal to the limiting pressure. All other solutions are identical concerning the upper frequency limit corresponding a wavelength obeying  $d = \lambda$ .

The limits for continuous available frequency bands due to residual sound pressure and due to weighting are gathered in Table 12 for two-element solutions. The best solutions in this sense are Approximation 6, Approximation 9 optimized upstream, and Approximation 10 optimized downstream. Approximations 7 and 8 with optimized delays are also good solutions in the sense that their

upper frequency limit is 1, that is, the frequency corresponding to the wavelength between the actuator elements.

*Table 11. Upper frequency limits of continuous available frequency bands of different three-element solutions in terms of  $d/\lambda$ , where  $\lambda$  corresponds the wavelength of the frequency limit.*

Solution	Highest available frequency $d/\lambda$
Ideal	1
Appr. 1	–
Appr. 2	1
Appr. 3	1
Appr. 4	1

Table 12. Upper frequency limits of continuous available frequency bands of different two-element solutions for different inter-channel delays.

Solution	Highest available frequency $d/\lambda$ when inter-channel delay optimized		
	downstream	upstream	no delay
Ideal	0.5	0.5	0.5
Appr. 5	–	0.39 <sup>*)</sup>	0.65
Appr. 6	–	–	–
Appr. 7	1	1	0.5
Appr. 8	1	1	0.5
Appr. 9	0.2 <sup>*)</sup>	–	0.5
Appr. 10	–	0.19 <sup>*)</sup>	0.5

<sup>\*)</sup> Not useful solutions

## 6. Digital control of unidirectional actuator systems

Active noise control systems are typically implemented using a digital signal processor [3, 35]. We now investigate the realization of the proposed unidirectional actuator systems where the frequency-dependent weightings and other control functions, such as the integrator and the delay elements, are approximated using linear digital filters. We present a number of design examples of digital control systems for unidirectional actuators. In these examples we assume that the diameter of the duct is 40 cm, and the lowest and highest frequencies of interest are 50 Hz and 900 Hz, respectively. The sampling frequency of the ANC system considered here is chosen to be 2.5 kHz. The highest frequency of operation (the Nyquist frequency) is thus 1.25 kHz. The distance between the two elements of the dipole source is assumed to be  $d = 0.3$  m in three-element systems and  $d = 0.15$  m in two-element systems.

### 6.1 Digital filter approximation of frequency-dependent weightings

The frequency-dependent weightings  $a$  and  $b$  needed for the monopole and dipole sources in many of the unidirectional actuator structures are zero-phase functions, i.e., real-valued functions of frequency. In other words, it is assumed that they do not bring about any extra delay to the acoustic signal. In practice, a digital filter always causes some delay that consists of a processing delay of one sampling interval plus a phase delay determined by the phase response of the filter. In addition it is necessary to take into account the delay caused by the AD and DA converters, anti-aliasing and reconstruction filters, and the loudspeakers. This total delay may be compensated by exploiting the initial propagation delay,  $\tau_L$  (see Figure 11, Figure 13, Figure 14, and Figure 15). In order to preserve causality, delay  $\tau_L$  must originally be large enough so that it is possible to extract the total processing delay from it. The practical implication is that the actuator must be sufficiently far away from the reference detector.

Since it is not desirable to cause any phase error in the filter approximations, we have chosen to use FIR (finite-length impulse response) filters as practical

weightings for the monopole and the dipole sources. It is well known that an FIR filter can be designed to have an exactly linear phase by forcing its impulse response to be symmetric [36], and furthermore, the delay caused by the filter can be forced to be an integral number of sampling intervals by choosing the length of the impulse response to be odd.

The linear-phase FIR filters bring about a delay of  $(L_{\text{FIR}} - 1)/2$  samples where  $L_{\text{FIR}}$  is the filter length. We must be careful not to use filters that are too long since this will risk the causality of the feedforward ANC systems. The propagation delay from the reference detector to the actuator must be larger than the processing delay of the digital control system — otherwise the system becomes non-causal and it cannot be used for broadband noise cancellation.

We use a weighted least-squares (WLS) method to design the coefficients of the FIR filter approximations (see, e.g., [36]). This method minimizes the squared weighted frequency response error. The WLS weighting function  $W$  (not to be confused with the monopole and dipole weighting functions  $a$  and  $b$ ) must have non-negative real values only. The value of  $W$  at each frequency determines the importance of the frequency response: if the weight is zero at any frequency, the ideal frequency response will not be approximated at all at that frequency. We use a small weight value (or zero) to neglect the specifications at very small frequencies (below 50 Hz) and at frequencies near the Nyquist frequency (above 900 Hz). In the frequency range of interest the weighting function may be unity or it may vary according to the ideal magnitude response specification.

The aim is to obtain digital filter approximations that do not restrict attenuation of the ANC system, i.e., the frequency response error of the FIR filters must be smaller than the typical attenuation obtainable with ANC systems (about 20 or 30 dB). Here we are mainly interested in the obtainable residual sound pressure downstream and the radiated sound pressure upstream. For Ideal Sources these figures should be much smaller than  $-20$  dB. We have chosen to aim at attenuation of at least 40 dB in the frequency band of interest (between 50 and 900 Hz).

### 6.1.1 Design example: weighting filter $b$ for Approximations 3 and 4

Figure 35 shows an example where the monopole weighting  $b$  for the unidirectional actuator Approximation 3 has been approximated using the WLS technique. The ideal magnitude response (solid curve in the upper part of the figure) has been computed according to Table 2, and coefficients for the linear-phase FIR filter of length 3 have been computed using a weighting function equal to 1 between 50 and 1000 Hz and zero elsewhere. The filter coefficients are  $h_b(0) = 0.2300$ ,  $h_b(1) = 0.5576$ , and  $h_b(2) = 0.2300$ .

The magnitude response of the FIR filter is plotted with a dashed line in the figure. The lower part of the figure illustrates the approximation error. The frequency response error has been computed as the absolute value of the difference of the ideal and approximate frequency responses. The largest frequency response error in the frequency band of interest (50 Hz ... 900 Hz) is in this case about  $-35$  dB.

The filter designed above may be used with the unidirectional actuator Approximation 4 as well, since there is only a minor difference between its magnitude response and that of Approximation 3. The sign of all the coefficients must be inverted and a constant 2 added to the middle coefficient ( $h_b(0) = -0.2300$ ,  $h_b(1) = 2 - 0.5576 = 1.4424$ , and  $h_b(2) = -0.2300$ ). The frequency response error is still the same as that illustrated in the lower part of Figure 35.

Note that it is practical to use short FIR filters to approximate the monopole and dipole weightings since long filters would bring about long delays as well as a large computational burden. The delay introduced by a linear-phase FIR filter is equal to the number of sampling intervals between the first and middle coefficient of the filter's impulse response. In the example of a 3-coefficient filter, the delay is 1 sample. At the sampling rate of  $f_s = 2.5$  kHz this corresponds to a distance of  $c_0/f_s = 0.137$  m (when  $c_0 = 343$  m/s). The causality constraint then requires that the distance from the reference microphone to the center point of the actuator is at least this much. Actually the distance must be larger due to the additional delay caused by processing, AD and DA converters, and the other system components.

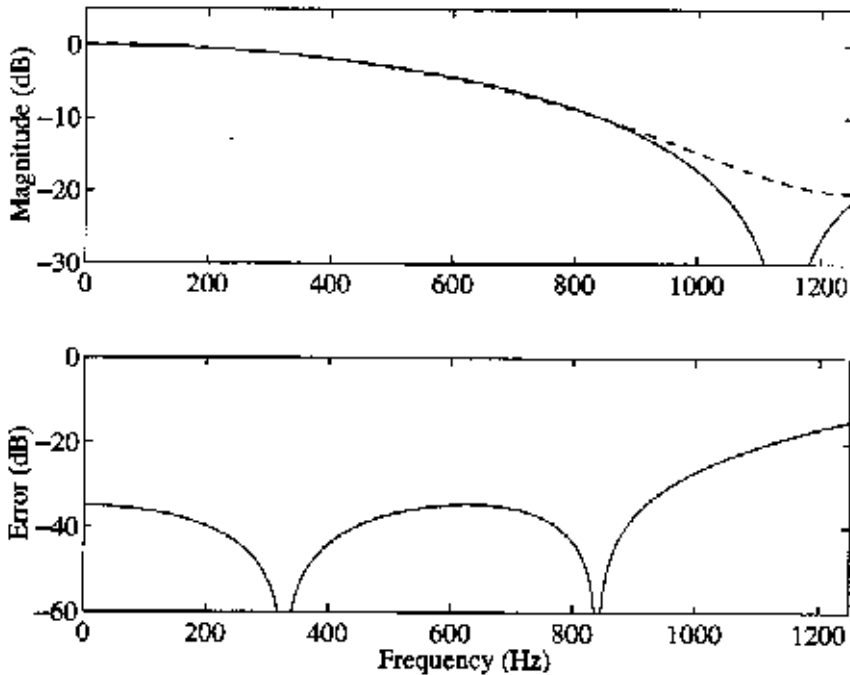


Figure 35. (Top) Magnitude response of the WLS FIR approximation (dashed line) of monopole weighting  $b$  (solid line) for Approximation 3. (Bottom) Frequency response error.

## 6.2 Digital integrator

### 6.2.1 Recursive feedback loop and FIR compensator

An integrator — scaled by a constant  $c_0/d$  — is needed in all the actuator systems described in this report (see Figure 11, Figure 13, Figure 14, and Figure 15) except for Approximation 6 optimized downstream. A good discrete-time approximation for an integrator is obtained by combining a feedback loop and an FIR compensator as discussed, e.g., in [37] and [38]. The transfer function of a scaled digital integrator needed in the unidirectional systems is

$$I(z) = \frac{c_0}{df_s} \frac{B_1(z)}{1 - a_1 z^{-r}}, \quad (22)$$

where  $c_0$  is the speed of sound in the fluid,  $d$  is the distance between the actuator elements,  $f_s$  is the sampling frequency,  $z$  is the complex variable used in Z-transforms,  $B_1(z)$  is the transfer function of the FIR compensator,  $a_1$  is a real-valued coefficient that must be slightly smaller than 1 to ensure stability, and  $r$  is the order of the feedback part (typical choices being  $r = 1$  or  $r = 2$ ). Choice  $r = 2$  yields a better approximation in the frequency band of interest, but the drawback is that then the filter has a pole at the Nyquist frequency with a very large  $Q$  value, which brings about a large gain at high frequencies.

Let us design a digital integrator consisting of a recursive feedback loop and an FIR compensator of length 5. We choose  $a_1 = 1 - 2^{-10} = 0.9990$  and  $r = 1$ . We set the WLS weighting function  $W$  to be equal to 1 between 0 and 900 Hz, and 0 above that. The magnitude and error responses are shown in Figure 36. The maximum error in the approximation band is about  $-26$  dB.

Approximations 3 and 4 have the integrator in their dipole control part and the monopole weighting may be realized using an FIR filter as discussed in the previous section. The sound pressure radiating downstream ( $p_+$ ) and upstream ( $p_-$ ) from a three-element actuator system may be evaluated using the following equations:

$$\begin{aligned} p_+ &= \frac{1}{2} \left[ 2 + \hat{a}\hat{l} (e^{-jkd/2} - e^{+jkd/2}) - \hat{b} \right] p_i e^{-jkx}, \quad x > +\frac{d}{2} \\ p_- &= \frac{1}{2} \left[ \hat{a}\hat{l} (e^{+jkd/2} - e^{-jkd/2}) - \hat{b} \right] p_i e^{+jkx}, \quad x < -\frac{d}{2}, \end{aligned} \quad (23)$$

which can be expressed also as

$$\begin{aligned} p_+ &= \frac{1}{2} \left[ 2 - 2j\hat{a}\hat{l} \sin(kd/2) - \hat{b} \right] p_i e^{-jkx}, \quad x > +\frac{d}{2} \\ p_- &= \frac{1}{2} \left[ 2j\hat{a}\hat{l} \sin(kd/2) - \hat{b} \right] p_i e^{+jkx}, \quad x < -\frac{d}{2}, \end{aligned} \quad (24)$$

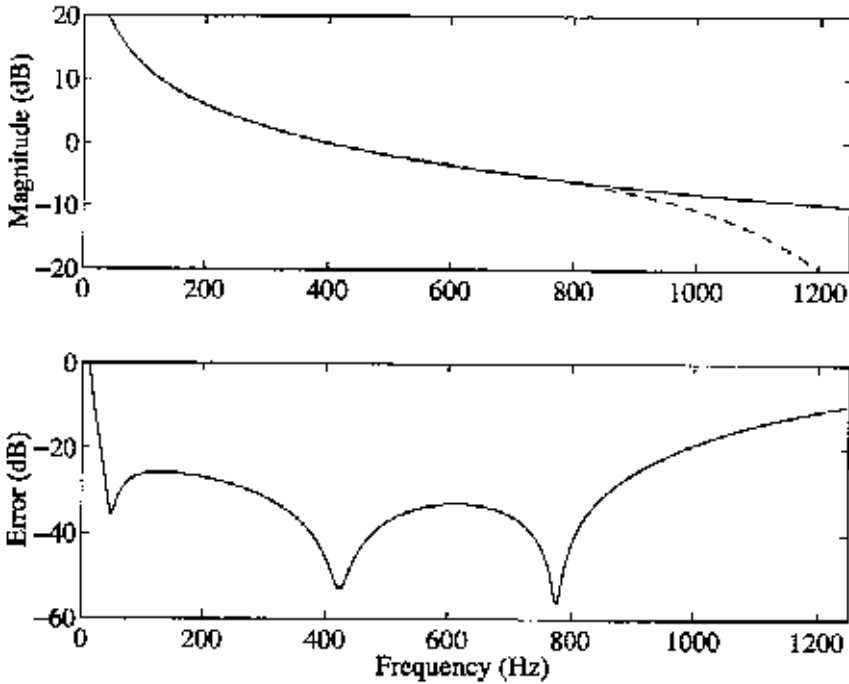


Figure 36. (Top) Magnitude response of the ideal integrator (solid line) and an example of its approximation using a digital filter (dashed line) and (Bottom) the corresponding frequency response error.

where  $\hat{a}$ ,  $\hat{b}$ , and  $\hat{I}$  are the frequency responses of the digital filter approximations of the dipole weighting  $a$ , monopole weighting  $b$ , and the integrator scaled by  $c_0/d$ , respectively.

An integrator with a length-7 FIR part, first-order feedback loop, and a length-5 monopole weighting FIR filter was designed for Approximation 3. The maximum sound pressure upstream with these digital filters is about than  $-43$  dB (assuming that the 3 actuator elements are perfect and there are no other faults in the system either) and the residual sound pressure downstream is similar (in the frequency range of interest) to the theoretic case shown in Figure 20 and Figure 21. For Approximation 4, the largest residual sound pressure downstream

is also less than  $-43$  dB and the maximum sound pressure upstream is nearly the same as the theoretic curve depicted in Figure 20 and Figure 21.

### 6.2.2 Combined approximation of the integrator and the dipole weighting

In some unidirectional actuator systems discussed in this report, a frequency-dependent dipole weighting function  $a$  together with the integrator is required in the dipole control path (see Figure 11, Figure 13, Figure 14, and Figure 15). This is the case for Ideal Sources and Approximations 2, 7, and 8. In these cases, we suggest *combining* the FIR compensator and the FIR approximation of  $a$ . This approach follows the general principle that it is better to perform all the approximations in one step rather than many approximations in series.

### 6.2.3 Design example: three-element Ideal Source

Let us approximate the combination of an integrator and the dipole weighting  $a$  for the unidirectional three-element Ideal Source (see Figure 11). We use a first-order feedback loop ( $r = 1$ ,  $a_I = 0.9990$ ) and an FIR filter with 13 coefficients. The delay caused by the filter is now about 6 samples, which corresponds to a propagation distance of about 0.8 meters. However, the delay is not exactly this, since now the impulse response of the FIR filter is not symmetric since it must correct both the magnitude and the *phase* response for the digital control of the dipole sources.

Figure 37 illustrates the magnitude responses (upper part of the figure) of the ideal transfer function and its approximation as well as the frequency response error (lower part of the figure). This result was obtained using a weighting function  $W$  in the WLS design that is 0 below 30 Hz, 1 between 10 and 600 Hz, 2 between 600 and 910 Hz and 0 above that. This weighting function was chosen because it was noticed that the errors near the upper edge of the frequency band of interest contributed strongly to the sound pressure radiated from three-element Ideal Source. The maximum frequency response error in the frequency band of interest is now about  $-26$  dB and we should again look at the obtainable attenuation downstream and radiation upstream.

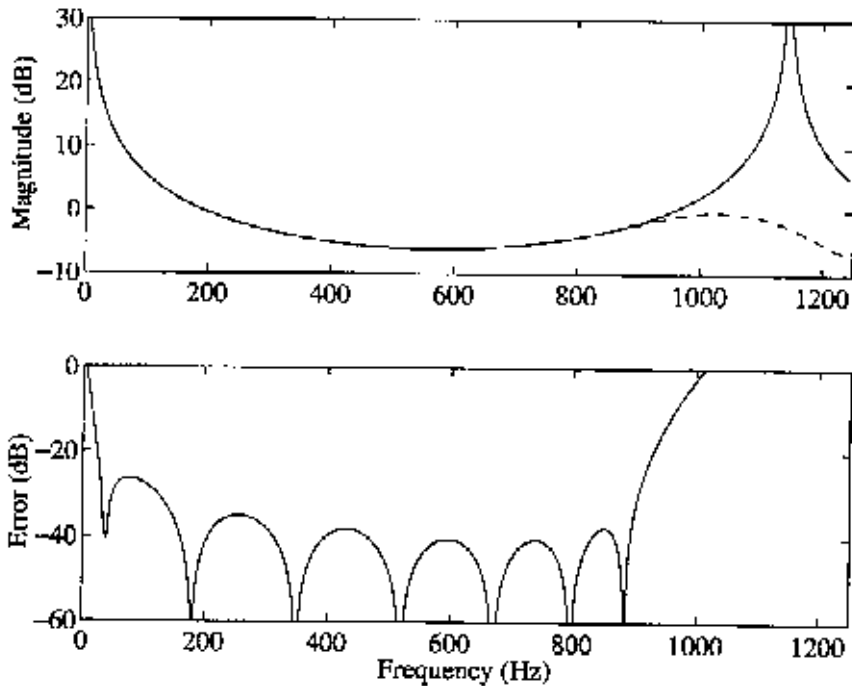


Figure 37. (Top) Magnitude response of the combination of an integrator and dipole weighting  $a$  for three-element Ideal Source (solid line) and its WLS FIR approximation (dashed line). (Bottom) Frequency response error. The distance between the dipole elements is  $d = 0.3$  m.

We evaluate the sound radiation upstream and downstream for three-element Ideal Source according to equation (23) to get a realistic estimate of how the approximation error due to digital filters affects the performance of the proposed ANC system. Note that when  $b = 1$ , the upstream and downstream radiation characteristics are equivalent (but in opposite phase). They are thus illustrated with a single curve in Figure 38. The maximum sound pressure in the specified frequency band is about  $-42$  dB. This is considered sufficient since it is more than what is usually obtained with practical active attenuation systems. Remember, however, that for Ideal Sources, the attenuation both up- and downstream is in theory infinite in dB.

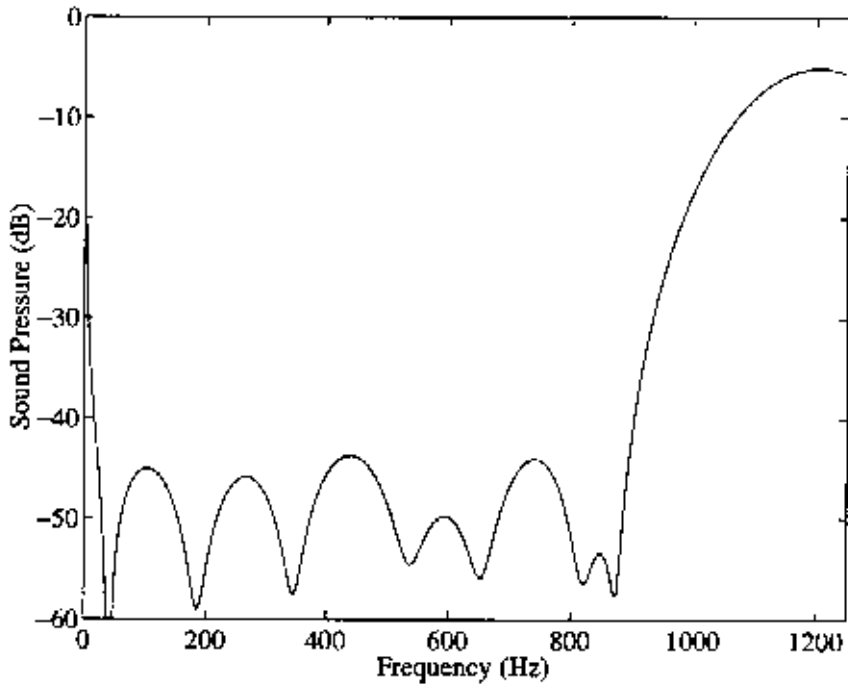


Figure 38. Sound radiation upstream and downstream from three-element Ideal Source when the integrator and dipole weighting have been approximated using a feedback loop and a single FIR filter with 13 coefficients.

### 6.3 Digital implementation of time delays

Three different propagation delays need to be realized in the proposed unidirectional actuator systems: the delay from the reference detector to the center point of the actuator (in all the systems of this report) and the delay  $\tau$  between the elements of the actuator and the delay  $\tau/2$  (in some two-element systems).

#### 6.3.1 Propagation delay

The propagation delay could be implemented as a fixed delay filter, but it is more common to use an adaptive filter that also takes into account losses or other filtering effects, such as dispersion, that may occur when sound pressure propagates in the duct. Another important reason for using an adaptive filter is

that the ANC system is then capable of tracking changes in the transfer function of cancellation path. The adaptive filter is often implemented using the well-known LMS algorithm (see, e.g., [35]). Winkler and Elliott describe the use of an adaptive FIR filter for modeling the propagation delay in cases of Swinbanks' source and maximal efficient two-element source [14]. Since this part of ANC systems is well understood and the use of a unidirectional actuator does not bring any considerable changes to it (apart from decreased acoustic feedback), this issue is not discussed further here.

### 6.3.2 Delay between actuator elements in two-element systems

The loudspeakers of the two-element actuator systems are located near each other (at distance  $d$ ) and in some structures the small delay  $\tau$  between them must be implemented as a delay filter (see Figure 6, Figure 13, and Figure 14). The complexity of implementing a delay filter depends essentially on the ratio of the delay time to the sampling interval  $T = 1/f_s$  where  $f_s$  is the sampling frequency used. If  $D = \tau/T$  is an integer, the delay can be implemented as a digital delay line of length  $D$ , that is, by simply delaying the digital signal by  $D$  sampling intervals. More generally,  $D = \tau/T$  is a real number with an integer and a real part. In the example case the distance between the centers of the two actuator elements is  $d = 0.15$  m and the desired delay in samples is  $D = 0.15 \text{ m} \times 2500 \text{ Hz} / 343 \text{ m/s} = 1.0933$ . The delay must now be modeled using a *fractional delay digital filter*. A review of such filter approximations has been carried out by Laakso *et al.* [39]. Fractional delay filters are implemented using discrete-time interpolation techniques.

In the context of Swinbanks' source and two-element maximal efficient source, Winkler and Elliott [14] discuss the influence of rounding the delay  $D$  to an integer value to be able to implement it as a digital delay line. They demonstrate that the downstream cancellation properties of the system are not seriously affected but that the sound radiation upstream then increases with frequency. Since we desire to develop an active noise control system that truly behaves unidirectionally, we study the use of fractional delay filters for maintaining also the downstream radiation near the theoretic minimum.

Let us consider how to realize the delay  $\tau$  needed in the control path of the monopole source (see Figure 13). The danger in using an FIR approximation for the

fractional delay is that the filter may have to be quite long. The causality of the system must be guaranteed by placing the reference detector still further away from the actuator system. Note that this is an additional constraint because the FIR filter approximation of weighting  $b$  also demands that the distance between the detector and actuator be sufficiently large. In order to achieve an adequately accurate delay filter with a small extra delay, we suggest the use of a *digital allpass filter* to approximate the fractional delay. It has been formerly noticed that the frequency response error achieved with allpass fractional delay filters is smaller than with FIR fractional delay filters when similar design criteria are used and the number of coefficients is the same (e.g., an allpass filter of order 5 is better than an FIR filter of length 10 when a similar design approach is used) [40].

We suggest using an allpass fractional delay filter that is an *equiripple* approximation of the ideal phase response. This design gives the best approximation in terms of maximum frequency response error in the approximation band. A very nearly equiripple approximation can be obtained with an iterative technique described by Laakso *et al.* [39]. Figure shows the phase delay and the frequency response error of a fifth-order equiripple allpass filter that approximates a delay of 5.0933 samples. The integer part of the delay is chosen to be 5 since it must be at least the allpass filter order minus one — otherwise the allpass filter becomes unstable. This filter causes an extra delay of 4 samples that corresponds to a propagation distance of 0.55 meters. The frequency response error shown in the lower part of the figure is the absolute difference of the frequency responses of the ideal delay of 5.0933 samples and the allpass filter. The maximum frequency response error in the approximation band (between 50 and 900 Hz) is about  $-56$  dB. This allpass filter is used in the next section for the two-element Swinbanks' source.

### 6.3.3 Delay $\tau/2$ in the control of the dipole control path in two-element systems

The delay of  $\tau/2$  needed in the control path of dipole elements (illustrated in Figure 13 and Figure 14) may be combined with the digital filter approximating the integrator and the weighting  $a$ , following the principle of a single-stage approximation. The filter may be designed using the WLS FIR filter design method as before.

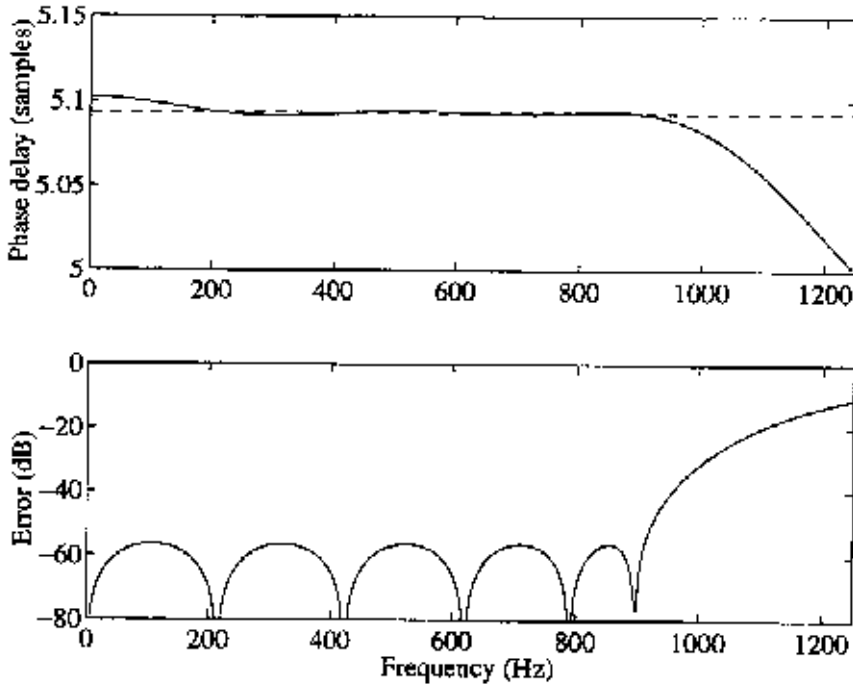


Figure 39. (Top) Phase delay response of the allpass filter of order 5 (solid line) approximating the constant phase delay of 5.0933 samples (dotted line). (Bottom) Corresponding frequency response error.

## 6.4 Design examples of two-element actuators

In addition to the control filters of three-element Ideal Source and Approximations 3 and 4 discussed above, we present the filters and obtainable attenuation for the two-element Swinbanks' source and the delayless Ideal Source, which are among the most promising unidirectional actuator systems.

### 6.4.1 Two-element Swinbanks' source

The weighting function of the two-element Swinbanks' structure must be implemented with an FIR filter of length 35 and a first-order feedback loop ( $a_1 = 0.9990$ ). The magnitude response of the ideal specification and the FIR filter are given in Figure 39. Also the frequency response error of approximation is dis-

played. The weighting function  $W$  used in the WLS design was unity between 120 and 600 Hz, 10 between 600 and 700 Hz, 30 between 700 and 900 Hz, and zero above that. This yielded an almost equiripple error curve in the approximation band with a maximum error of about  $-42$  dB.

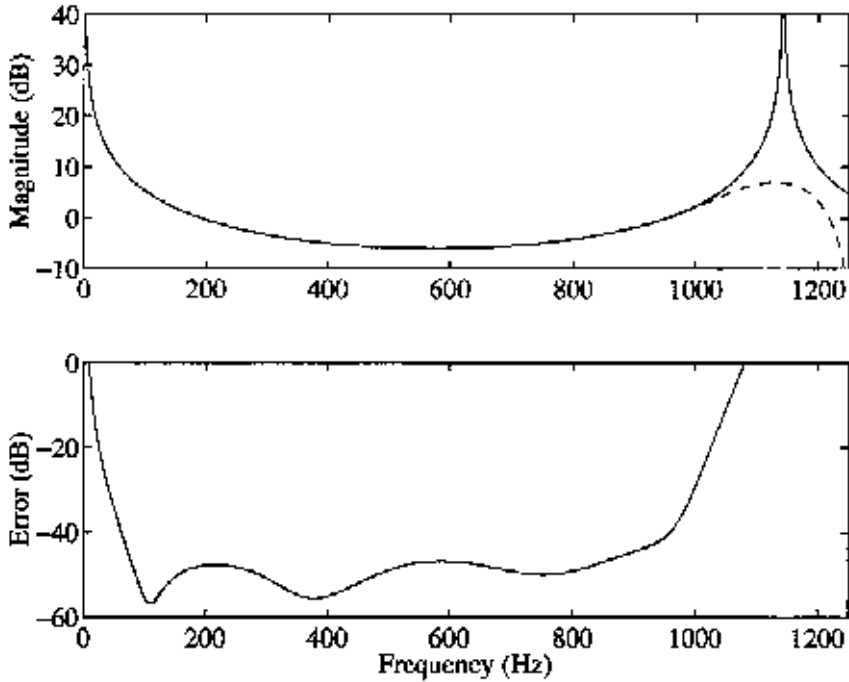


Figure 39. (Top) Magnitude response of the weighting function  $IA/2$  for the two-element Swinbanks' source (solid line) and its FIR filter approximation (dashed line). (Bottom) The corresponding frequency response error.

We evaluate the obtainable attenuation by using the equations for the sound pressure radiating downstream ( $p_+$ ) and upstream ( $p_-$ ) from the two-element Swinbanks' system:

$$\begin{aligned}
 p_+ &= \left[ 1 + \frac{1}{2} \hat{I}\hat{A}(\hat{F}_d - e^{+jkd}) \right] p_i e^{-jkx}, \quad x > +\frac{d}{2} \\
 p_- &= \frac{1}{2} \hat{I}\hat{A}(\hat{F}_d e^{+jkd} - 1) p_i e^{+jkx}, \quad x < -\frac{d}{2},
 \end{aligned} \tag{25}$$

where  $\hat{A}/2$  is the approximation of the Swinbanks' weighting function, which has now been realized with a single digital filter, and  $\hat{F}_d$  is the frequency response of the allpass fractional delay filter.

Figure 40 shows the residual level downstream (solid line) and upstream (dashed line), when the two-element Swinbanks' source has been implemented with the combined filter of Figure 39 and the allpass filter of Figure . The attenuation both down- and upstream is now better than 40 dB in the approximation band. Note, however, that at many frequencies, the upstream attenuation is much better than what was required. A more sophisticated filter design algorithm could account for this and thus it could be possible to obtain the needed attenuation with a lower order filter approximation of the Swinbanks' weighting.

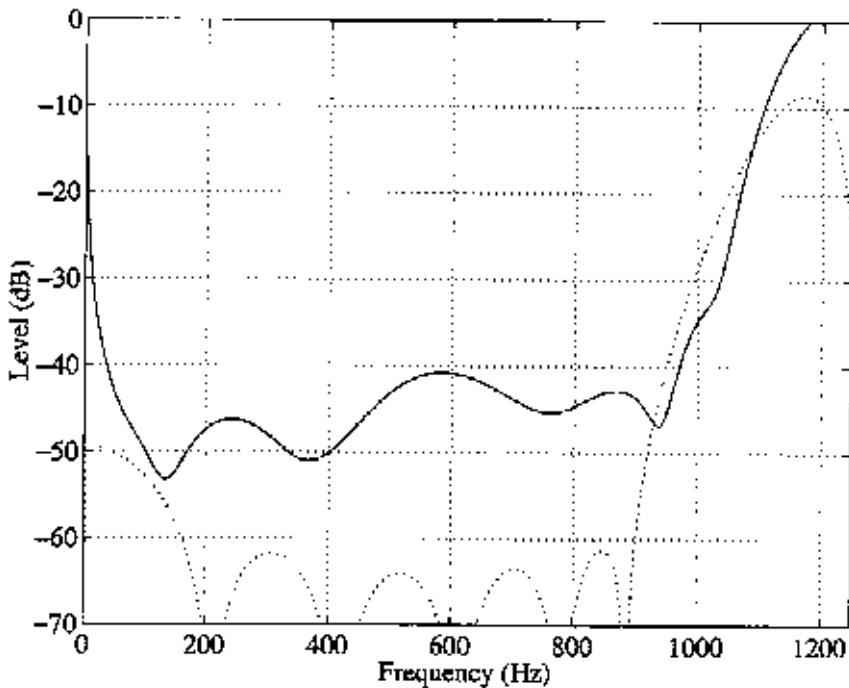


Figure 40. Sound radiation downstream (solid line) and upstream (dashed line) from Swinbanks' two-element source.

The filters used in this design example — an FIR filter of length 35 and an all-pass filter of order 5 — together cause a very long delay: 17 samples due to the FIR and 4 samples due to the allpass filter (remember that the required delay to be produced by the allpass filter was 1.0933), or 21 samples. This corresponds to a propagation distance of 2.88 meters. This is the minimum distance between the reference microphone and the actuator in a duct-ANC application.

### 6.4.2 Delayless two-element Ideal Source

Our final design example concerns delayless two-element Ideal Source presented in Figure 15. This structure may be implemented with two control filters, one approximating weighting  $-b/2$  and the other the combination of a scaled integrator and weighting  $a$ . The formulae for weighting functions  $a$  and  $b$  are available in Table 7.

Figure 41 shows the magnitude response of the combination of the integrator and function  $a$  as well as their filter approximation (FIR part of length 11 and a second-order feedback loop with  $a_1 = 0.9990$ ). The weighting function  $W$  in the filter design was unity between 40 and 920 Hz and zero elsewhere. It is seen that the frequency response error is smaller than  $-40$  dB in the approximation band (50...900 Hz) (see lower part of Figure 41). Figure 42 presents the magnitude responses (upper part of the figure) of weighting  $-b/2$  and its FIR approximation of length 11 and the frequency response error (lower part). In this case the weighting function  $W$  was proportional to the absolute value of  $b$  at the frequency band 100...950 Hz and zero elsewhere. Also now, the error is smaller than  $-40$  dB.

Finally, we evaluate the obtainable attenuation by using the equations for the sound pressure radiating downstream ( $p_+$ ) and upstream ( $p_-$ ) from the two-element delayless Ideal Source:

$$\begin{aligned}
p_+ &= \frac{1}{2} \left[ 2 + \hat{a}\hat{I}(e^{-jkd/2} - e^{+jkd/2}) - \frac{\hat{b}}{2}(e^{-jkd/2} + e^{+jkd/2}) \right] p_i e^{-jkx} , \quad x > +\frac{d}{2} \\
p_- &= \frac{1}{2} \left[ \hat{a}\hat{I}(e^{+jkd/2} - e^{-jkd/2}) - \frac{\hat{b}}{2}(e^{+jkd/2} + e^{-jkd/2}) \right] p_i e^{+jkx} , \quad x < -\frac{d}{2} ,
\end{aligned} \tag{26}$$

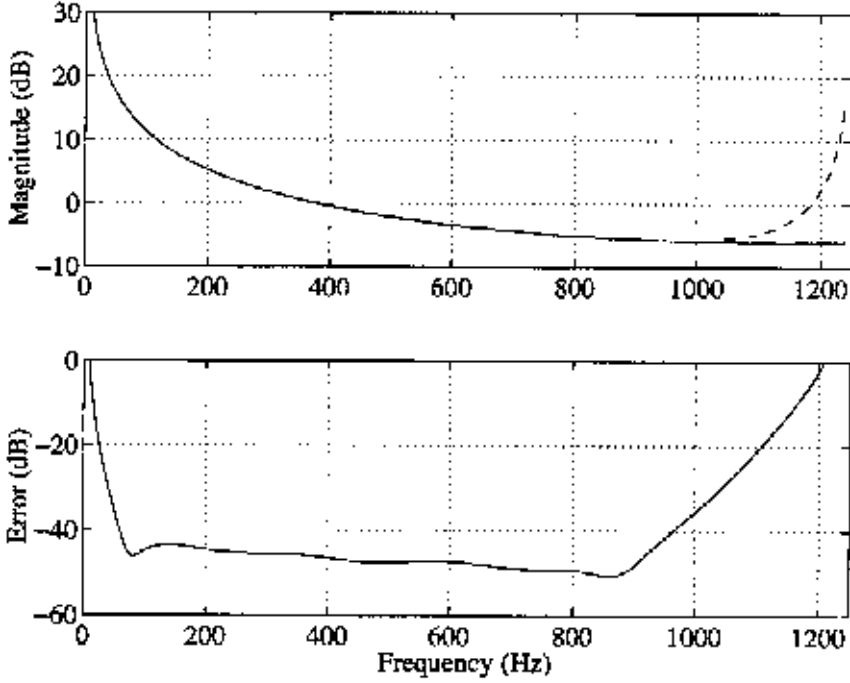


Figure 41. (Top) Magnitude response of the combination of the integrator and weighting  $a$  of two-element delayless Ideal Source (solid line) and its approximation (dashed line) and (bottom) the corresponding frequency response error.

which can also be presented as

$$\begin{aligned}
p_+ &= \frac{1}{2} \left[ 2 - 2j\hat{a}\hat{I} \sin(kd/2) - \hat{b} \cos(kd/2) \right] p_i e^{-jkx} , \quad x > +\frac{d}{2} \\
p_- &= \frac{1}{2} \left[ 2j\hat{a}\hat{I} \sin(kd/2) - \hat{b} \cos(kd/2) \right] p_i e^{+jkx} , \quad x < -\frac{d}{2} .
\end{aligned} \tag{27}$$

The residual pressure level as a function of frequency is shown in Figure 43. It is seen that the level is smaller than  $-40$  dB in the approximation band both down- (solid line) and upstream (dashed line) as required.

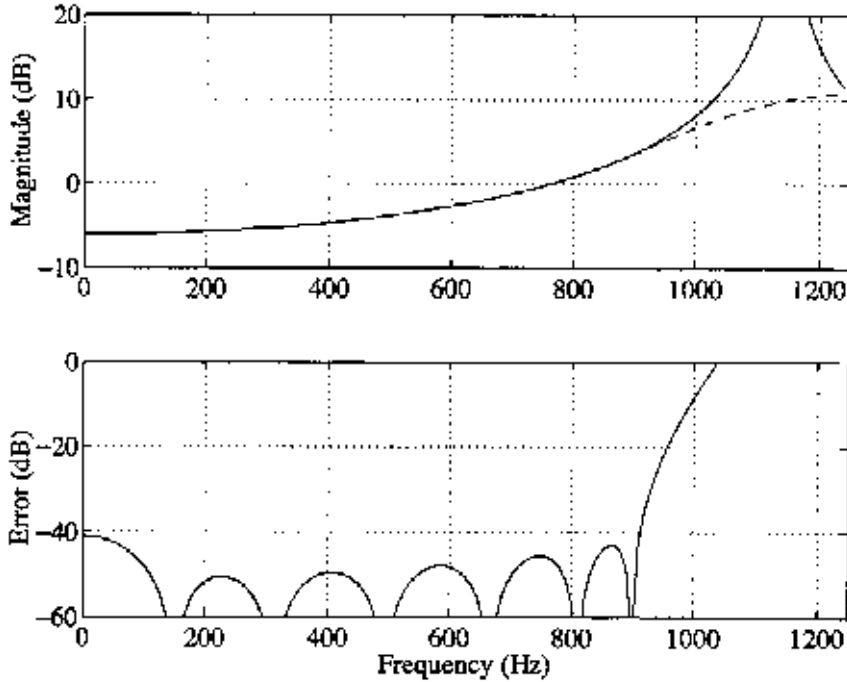


Figure 42. (Top) Magnitude response of weighting function  $-b/2$  of two-element delayless Ideal Source (solid line) and its FIR approximation (dashed line) and (bottom) the corresponding frequency response error.

The FIR filters used to implement the delayless two-element source in this example were of length 11. This filter length causes a delay of 5 samples, which is equivalent to a propagation delay of 0.69 meters. This example shows that a compact implementation of delayless two-element Ideal Source is feasible. Remember that the traditional two-element Swinbanks' structure requires a distance of 2.9 meters to fulfill the same attenuation specifications. Thus, it is recommended to use the new delayless structure instead in the future.

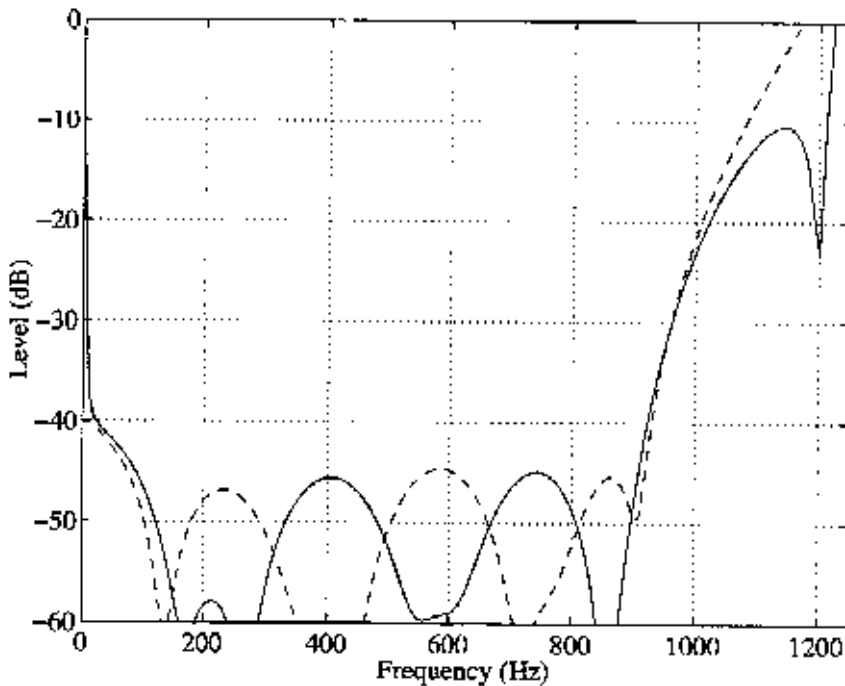


Figure 43. Sound radiation downstream (solid line) and upstream (dashed line) from the delayless two-element Ideal Source when the control filters are implemented as digital filters. The distance between the two actuator elements is  $d = 0.15$  m.

## 6.5 Implementation issues

In the design examples we have assumed that the two or three actuators used are ideal in the sense that their frequency response is flat and they cause no delay. In practice the frequency responses of loudspeakers vary considerably at difference frequencies, they cause phase delay, and the properties of any two loudspeakers are different. This implies that in practice it is necessary to equalize the actuators. This may be done by measuring the impulse response and designing an inverse filter to be used to preprocess the input signal of the actuator. Another choice is to use an adaptive filter for equalization.

The transfer function from the reference detector to the actuator system may be estimated and implemented with an adaptive filter, as is usually done in current active noise control systems. Other control functions required in unidirectional actuator structures may be realized with fixed digital filters.

## **6.6 Discussion of digital control**

We have now designed a number of digital filters to control some of the unidirectional actuator systems. A general conclusion is that there are three- and two-element systems that can be implemented efficiently using digital control. When three-element Ideal Source or delayless two-element Ideal Source structure is used, relatively low-order digital filters enable good attenuation downstream and weak upstream radiation. A compact active attenuation system may be built where the distance between the reference actuator and the canceling actuator structure is less than a meter.

In contrast, some of the two-element systems present difficulties. Particularly, it was shown by example that the traditional two-element Swinbanks' source is not very well suited to practical implementation since it requires a long control filter. In our example, the FIR filter length had to be 35 in order to achieve an attenuation of 40 dB both down- and upstream. This implies that the distance between the reference detector and the actuator structure must be almost 3 meters. This may be impractical in an ANC application. In light of the theory presented earlier in this report and the design examples of this section, we can recommend the use of the three-element Ideal Source and the delayless two-element Ideal Source.

## 7. Conclusions

We have given a review of three- and two-element unidirectional actuator structures for feedforward active noise control in a duct. All the actuator systems presented in this report were derived from the JMC source, an ideal unidirectional source consisting of an ideal monopole and an ideal dipole, which is difficult to realize.

Practical realization of a *three-element* JMC source in a duct requires three monopole sources, two of which are in opposite phase to construct a dipole, while the third monopole source is located between the two. The input signals of the dipole and monopole elements have to be filtered to achieve good attenuation downstream and upstream. By systematically modifying the frequency-dependent weightings of the three-element JMC source, we have found a realization for a new perfect unidirectional three-element actuator (the three-element Ideal Source) and four different ways to approximate it (Approximations 1 – 4), also new solutions. The weighting functions for the different structures are gathered in Table 2, and the residual sound pressures down- and upstream in Table 3. Three-element Ideal Source provides a novel approach to implement a unidirectional actuator that completely absorbs the downstream sound pressure and causes no upstream radiation. Three-element Approximation 2 is a three-element generalization of the maximally efficient two-element source recently defined by Winkler and Elliott [14]. It is not unidirectional at low frequencies, but the downstream radiation is totally canceled. Approximation 3 has a non-zero downstream residual sound pressure, Approximation 4 has a non-zero upstream residual sound pressure, and Approximation 1 has non-zero residual sound pressures in both directions.

The unidirectional JMC source may also be realized as a *two-element* source, and approximated with two monopole sources by combining the contribution of one monopole element—the middle one in the original three-element configuration—with the element pair that constitutes the dipole. By using appropriate control functions, we managed to find one perfect unidirectional configuration (two-element Ideal Source) and six approximations (5 – 10) that use two loudspeaker elements. Additionally, there are three ways to choose the delay between the two channels: the delay may be optimized downstream or upstream or the delay can be removed altogether. The two-element Ideal Source and Ap-

proximations 5 – 10 for all three inter-channel delays are new JMC-based two-element unidirectional sources to be applied in ducts. The only exception is Approximation 6 (maximally efficient source) with the inter-channel delay optimized downstream, which is the same as the maximally efficient source of Winkler and Elliott [14]. The drawback of the maximally efficient source is that it does not completely eliminate upstream radiation at low frequencies. Approximations 6 (the maximally efficient source), 8, and 10 perfectly cancel the sound pressure downstream but not so well upstream. Approximations 7 and 9 cancel the downstream wave but they do not suppress the upstream radiation well.

The three inter-channel delay optimization schemes offer 20 new two-element structures that may be used for implementing a unidirectional actuator for active noise control in a duct. Control structures for the two-element structures were derived and their properties were compared. The weighting functions for the different structures are gathered in Table 5, Table 6, and Table 7, and the residual sound pressures down- and upstream in Table 8, Table 9, and Table 10. Furthermore, implementation of digital control structures for the actuator systems was discussed.

The output volume velocities of all the three variations of two-element Ideal Source are mutually identical and independent of the inter-channel delay optimization: the differences in the weighting functions compensate the differences in the delays. The volume velocities are also identical with those of Swinbanks' two-element actuator [15], although the procedure of attaining them is quite different. The control system of the Swinbanks' two-element actuator may seem simple in relation to those of two-element Ideal Source. However, the delayless version of two-element Ideal Source has the advantage of no separate phase shift between the volume velocities of the elements, which turns out to be advantageous in the practical implementation of digital control systems.

With the three-element solutions, except with Approximation 2, the available frequency band is limited by an upper frequency corresponding a wavelength that obeys  $d = \lambda$  (Approximation 1 can be used at a little higher frequencies). With the two-element solutions, the available frequency range depends on the singularities of the weighting function and the radiation properties of the unidirectional actuator system. Approximation 6 has no frequency limitations what-

soever. Also Approximation 5 optimized downstream, Approximation 9 optimized upstream and Approximation 10 optimized downstream have an unlimited frequency range. The highest frequency of Approximation 5 without inter-channel delay corresponds to about 65 % of  $d/\lambda$ . In this respect the delayless structures seem to be advantageous since all the other structures (except for Approximations 5 and 6) have an upper frequency limit of  $d/2\lambda$ , which is considered good for practical realizations.

Choosing the best unidirectional actuator structure is not trivial. The main issues to be taken into account are the obtainable attenuation both down- and upstream, the available frequency band, and the complexity of the implementation of the control system. Only Ideal Sources enable perfect cancellation of radiated sound in both directions. The fact that the unidirectional solutions based on the JMC method can be realized without inter-channel delays makes these solutions superior to all other solutions, e.g., that of Swinbanks [15], Berengier and Roure [17], and La Fontaine and Shepherd [18]. In the digital realization of the control system, the short delays require much signal processing power. With the JMC-based solutions it is possible to achieve simplified control algorithms and reduce the computing time or improve the performance. The three-element Ideal Source and the delayless two-element Ideal Source thus seem to be the best choices for practical ANC work in ducts.

Future research in the area of unidirectional actuators for ducts will include practical implementation and measurements with the new actuator configurations. It seems feasible to implement the control functions of the loudspeaker elements and the adaptive filtering with one signal processor. This is especially likely because the use of a unidirectional actuator system makes it unnecessary to use adaptive IIR filters or other signal processing methods to cancel the acoustic feedback. It may be necessary to correct any irregularities in the frequency responses of the loudspeaker elements by means of digital signal processing (inverse filtering), since in principle the loudspeaker elements should have identical, flat frequency responses. This implies that the frequency response of each loudspeaker element has to be measured and a difference between its "ideal" or desired frequency response be determined. The inverse of this error frequency response may be included in the specification of the control filter of the loudspeaker element.

The unidirectional systems described in this report can be used for realizing reference detectors as well. The combined use of a unidirectional actuator and a unidirectional detector seems to be an effective way to minimize the acoustic feedback in tube-acoustic ANC systems. This strategy deserves closer examination in the future.

## References

1. Doak, P. E. Excitation, transmission and radiation of sound from source distributions in hard-walled ducts of finite length (I): The effects of duct cross-section geometry and source distribution space-time pattern. *J. Sound Vib.* 1973. Vol. 31, no. 1, pp. 1-72.
2. Doak, P. E. Excitation, transmission and radiation of sound from source distributions in hard-walled ducts of finite length (II): The effects of duct length. *J. Sound. Vib.* 1973. Vol. 31, no. 2, pp. 137-174.
3. Nelson, P. A. & Elliott, S. J. *Active control of sound*. London: Academic Press, 1992. 436 p. ISBN 0-12-515426-7
4. La Fontaine, R. F. & Shepherd, I. C. The influence of waveguide reflections and system configuration on the performance of an active noise attenuator. *J. Sound Vib.* 1985. Vol. 100, no. 4, pp. 569-579.
5. Ross, C. F. An algorithm for designing a broadband active sound control system. *J. Sound Vib.* 1982. Vol. 80, no. 3, pp. 373-380.
6. Ross, C. F. An adaptive digital filter for broadband active sound control. *J. Sound Vib.* 1982. Vol. 80, no. 3, pp. 381-388.
7. Eriksson, L. J., Allie, M. C. & Greiner, R. A. The selection and application of an IIR adaptive filter for use in active sound attenuation. *IEEE Trans. Acoust., Speech and Signal Processing* 1987. Vol. 35, no. 4, pp. 433-437.
8. Eghtesadi, Kh. & Leventhall, H. G. Active attenuation of noise — the monopole system. *J. Acoust. Soc. Am.* 1982. Vol. 71, no. 3, pp. 608-611.
9. Eghtesadi, Kh., Hong, W. K. W. & Leventhall, H. G. The tight-coupled monopole active attenuator in a duct. *Noise Control Eng. J.* 1983. Vol. 19, no. 1, pp. 16-20.

10. Zhou, J. & Shi, T. A study of the analogue compensating monopole system for active attenuation of noise in a duct. *Applied Acoustics* 1989. Vol. 28, no. 3, pp. 187-202.
11. Eghtesadi, Kh. & Leventhall, H. G. Active attenuation of noise: the Chelsea dipole. *J. Sound Vib.* 1981. Vol. 75, no. 1, pp. 127-134.
12. Hamada, H., Miura, T., Takahashi, M. & Oguri, Y. Adaptive noise control system in air-conditioning ducts. *Inter-Noise 88, proceedings.* Avignon, France 1988. Pp. 1017-1020.
13. Kuo, S. M. & Tsai, J. Acoustical mechanisms and performance of various active duct noise control systems. *Applied Acoustics* 1994. Vol. 41, no.1, pp. 81-91.
14. Winkler, J. & Elliott, S. J. Adaptive control of broadband sound in ducts using a pair of loudspeakers. *Acustica* 1995. Vol. 81, no. 5, pp. 475-488.
15. Swinbanks, M. A. The active control of sound propagation in long ducts. *J. Sound Vib.* 1973. Vol. 27, no. 3, pp. 411-436.
16. Poole, J. H. B. & Leventhall, H. G. An experimental study of Swinbanks' method of active attenuation of sound in ducts. *J. Sound Vib.* 1976. Vol. 49, no. 2, pp. 257-266.
17. Berengier, M. & Roure, A. Broad-band active sound absorption in a duct carrying uniformly flowing fluid. *J. Sound Vib.* 1980. Vol. 68, no. 3, pp. 437-449.
18. La Fontaine, R. F. & Shepherd, I. C. An experimental study of a broadband active attenuator for cancellation of random noise in ducts. *J. Sound Vib.* 1983. Vol. 91, no. 3, pp. 351-362.
19. Kazakia, J. Y. A study of active attenuation of broadband noise. *J. Sound Vib.* 1986. Vol. 110, no. 3, pp. 495-509.

20. Eghtesadi, Kh. & Leventhall, H. G. A study of  $n$ -source active attenuator arrays for noise in ducts. *J. Sound Vib.* 1983. Vol. 91, no. 1, pp. 11-19.
21. Guicking, D. & Freienstein, H. Broadband active sound absorption in ducts with thinned loudspeaker arrays. *Active 95, proceedings.* Newport Beach, California 1995. Pp. 371-382.
22. Mangiante, G. Active sound absorption. *J. Acoust. Soc. Amer.* 1977. Vol 61, no. 6, pp. 1516-1523.
23. Jessel, M. & Angevine, O. Active acoustic attenuation of a complex noise source. *Inter-Noise 80, proceedings.* Miami, Florida 1980. Pp. 689-694.
24. Jessel, M. J. M. Active noise reduction as an experimental application of the general system theory. *Inter-Noise 83, proceedings.* Edinburgh, Scotland 1983. Pp. 411-414.
25. Resconi, G. & Jessel, M. A general system logical theory. *Int. J. General Systems.* 1986. Vol. 12, pp. 159-182.
26. Illényi, A. & Jessel, M. Decoding/recoding the source information from/into sound fields: another way of understanding active noise control. *Inter-Noise 88, proceedings.* Avignon, France 1988. Pp. 963-966.
27. Jessel, M. J. M. 25 years with active noise control / a survey and comments with reference to Guicking's bibliography and "field reshaping" theory. *Inter-Noise 88, proceedings.* Avignon, France 1988. Pp. 953-958.
28. Mangiante, G. Active noise control in a duct: the JMC method. *Inter-Noise 90, proceedings.* Gothenburg, Sweden 1990. Pp. 1297-1300.
29. Uosukainen, S. Modified JMC method in active control of sound. *Acustica united with acta acustica* 1997. Vol. 83, no. 1, pp. 105-112.
30. Jessel, M. J. M. & Mangiante, G. A. Active sound absorbers in an air duct. *J. Sound Vib.* 1972. Vol 23, no. 3, pp. 383-390.

31. Canévet, G. & Mangiante, G. Absorption acoustique active et anti-bruit à une dimension. *Acustica* 1974. Vol. 30, pp. 40-48.
32. Canévet, G. Active sound absorption in an air conditioning duct. *J. Sound Vib.* 1978. Vol. 58, no. 3, pp. 333-345.
33. Boone, M. M. & Ouweltjes, O. Design of a loudspeaker system with a low-frequency cardioidlike radiation pattern. *J. Audio Eng. Soc.* 1997. Vol. 45, no. 9, pp. 702-707.
34. Elliott, S. J. A simple two microphone method of measuring absorption coefficient. *Acoustics Letters* 1981. Vol. 5, no. 2, pp. 39-44.
35. Kuo, S. M. & Morgan, D. R. *Active noise control systems: algorithms and DSP implementations*. New York: Wiley, 1996. 389 p. ISBN 0-471-13424-4
36. Parks, T. W. & Burrus, C. S. *Digital filter design*. New York: Wiley, 1987. 342 p. ISBN 0-471-82896-3
37. Abed, A. H. M., Bloom, P. J. & Cain, G. D. Digital integrators using optimal FIR compensators. *IEEE Trans. Acoustics, Speech and Signal Processing* 1983. Vol. 31, no. 3, pp. 726-729.
38. Papamarkos, N. & Chamzas, C. A new approach for the design of digital integrators. *IEEE Trans. Signal Processing* 1996. Vol. 43, no. 9, pp. 785-791.
39. Laakso, T. I., Välimäki, V., Karjalainen, M. & Laine, U. K. Splitting the unit delay — tools for fractional delay filter design. *IEEE Signal Processing Magazine* 1996. Vol. 13, no. 1, pp. 30-60.
40. Välimäki, V. & Laakso, T. I. Splitting the unit delay — digital filter approximations for fractional delay. 1996 *IEEE Nordic Signal Processing Symposium, proceedings*. Espoo, Finland 1996. Pp. 479-482.

## Appendix A: Derivations of frequency-dependent weighting functions for the three-element JMC actuators

In this Appendix the values of the weighting functions  $a$  and  $b$ , presented in Figure 11, for the three-element JMC actuators are derived. Also in this Appendix are presented the general relationships for the weighting functions for three special cases: the radiation upstream will not exceed a limiting value, the total sound downstream will not exceed a limiting value, and the case where there is a requirement for the ratio of the upstream and downstream sound pressures.

Without any weightings, the total sound pressure downstream and the sound radiated upstream can be obtained by the help of equations (10) and (11) in the form as with Approximation 1 presented in Table 3. With weighting functions, the total sound pressure downstream ( $p_+$ ) and the sound radiated by the actuator upstream ( $p_-$ ) are according to equations (12) and (13)

$$\begin{aligned} p_+ &= \frac{1}{2} \left( 2 - a \frac{\sin(kd/2)}{kd/2} - b \right) p_i e^{-jkx} \quad , \quad x > +\frac{d}{2} \\ p_- &= \frac{1}{2} \left( a \frac{\sin(kd/2)}{kd/2} - b \right) p_i e^{+jkx} \quad , \quad x < -\frac{d}{2} \end{aligned} \quad (A1)$$

### Condition for unidirectionality

If it is required that the actuator will *not radiate sound upstream*, the following equation has to be fulfilled

$$a \frac{\sin(kd/2)}{kd/2} = b \quad . \quad (A2)$$

In this case the total sound pressure downstream is

$$p_+ = (1 - b) p_i e^{-jkx} \quad . \quad (A3)$$

## Condition for total cancellation downstream

If it is required that the *total sound pressure downstream will vanish*, the following equation has to be fulfilled

$$a \frac{\sin(kd / 2)}{kd / 2} + b = 2 . \quad (\text{A4})$$

In that case the sound pressure upstream, radiated by the actuator, is

$$p_- = (1 - b) p_i e^{+jkx} . \quad (\text{A5})$$

## Effort of the actuator

The squared sum of the absolute values of the volume velocities, defined by equations (12) and (13), can be written, using equation (A4), as

$$\sum_k |q_k|^2 = \frac{1}{8} \left( 2|b|^2 + \frac{4 - 4 \operatorname{Re}\{b\} + |b|^2}{\sin^2(kd / 2)} \right) |q_i|^2 , \quad (\text{A6})$$

where  $\operatorname{Re}\{\cdot\}$  denotes the real part. If the derivatives of this expression attached to variables  $\operatorname{Re}\{b\}$  and  $\operatorname{Im}\{b\}$  (where  $\operatorname{Im}\{\cdot\}$  denotes the imaginary part) are required to vanish, one obtains the weightings of the *maximally efficient three-element source*.

## Limiting value conditions

If it is required that the *radiation upstream will not exceed a limiting value*

$$|p_-| \leq \frac{|p_i|}{c_1} , \quad (\text{A7})$$

the weightings must obey

$$\left| a \frac{\sin(kd / 2)}{kd / 2} - b \right| \leq \frac{2}{c_1} . \quad (\text{A8})$$

If it is required that the *total sound downstream will not exceed a limiting value*

$$\left| p_+ \right| \leq \frac{|p_i|}{c_2} , \quad (\text{A9})$$

the weightings must obey

$$\left| 2 - a \frac{\sin(kd / 2)}{kd / 2} - b \right| \leq \frac{2}{c_2} . \quad (\text{A10})$$

### Ratio condition

If there is a requirement for the *ratio of upstream to downstream sound pressures*

$$\frac{p_- e^{-jkx}}{p_+ e^{+jkx}} = c , \quad (\text{A11})$$

where the ratio  $c$  can be a complex-valued function of frequency, the relation between weightings  $a$  and  $b$  can be written, according to equation (A1), as

$$a(1 + c) \frac{\sin(kd / 2)}{kd / 2} - b(1 - c) = 2c . \quad (\text{A12})$$

This kind of requirement may be useful when optimizing the total efficiency of a detector-actuator system. The optimum value of  $c$  for the actuator depends on the directional characteristics of the detector (how sensitive the detector is to the acoustic feedback).

In this case the total sound pressure downstream and the sound pressure upstream are

$$\begin{aligned}
p_+ &= \frac{1}{1+c} (1-b) p_i e^{-jkx} \quad , \quad x > +\frac{d}{2} \\
p_- &= \frac{c}{1+c} (1-b) p_i e^{+jkx} \quad , \quad x < -\frac{d}{2} \quad .
\end{aligned}
\tag{A13}$$

If the monopole is not modified ( $b = 1$ ), according to equation (A12) three-element Ideal Source is obtained. If the dipole is not modified ( $a = 1$ ), according to equation (A12) weighting  $b$  can be written as

$$b = \frac{1}{1-c} \left( (1+c) \frac{\sin(kd/2)}{kd/2} - 2c \right) .
\tag{A14}$$

The total sound pressure downstream and the sound pressure upstream are as in equation (A13), and they can be also presented as

$$\begin{aligned}
p_+ &= \frac{1}{1-c} \left( 1 - \frac{\sin(kd/2)}{kd/2} \right) p_i e^{-jkx} \\
p_- &= \frac{c}{1-c} \left( 1 - \frac{\sin(kd/2)}{kd/2} \right) p_i e^{+jkx} \quad .
\end{aligned}
\tag{A15}$$

If the ratio is selected as  $c = -1$ , it corresponds to the situation of no weighting. In that case the magnitudes of the downstream and upstream sound pressures are the same.

## Appendix B: Derivations of frequency-dependent weighting functions for the two-element JMC actuators

In this Appendix the values of the weighting functions  $a$  and  $b$ , presented in Figure 13, Figure 14, and Figure 15, for the two-element JMC actuators are derived. Also in this Appendix are presented the general relationships for the weighting functions for three special cases: the radiation upstream will not exceed a limiting value, the total sound downstream will not exceed a limiting value, and the case where there is a requirement for the ratio of the upstream and downstream sound pressures.

Without any weightings, the total sound pressure downstream and the sound radiated upstream can be obtained by the help of equations (15), (16), or (17) in the form as with Approximation 5 presented in Table 8, Table 9, or Table 10. The various alternatives correspond to cases where the inter-channel delay is optimized downstream, upstream or where there is no inter-channel delay, respectively. With weighting functions, the total sound pressure downstream ( $p_+$ ) and the sound radiated by the actuator upstream ( $p_-$ ) are according to equations (18), (19), and (20)

Delay optimized:	$\frac{P_+}{p_i e^{-jkx}} =$	$\frac{P_-}{p_i e^{+jkx}} =$
downstream	$\frac{1}{2} \left( 2 - a \frac{\sin(kd/2)}{kd/2} - b \right)$	$\frac{1}{2} \left( a \frac{\sin(kd/2)}{kd/2} - b \cos(kd) \right)$
upstream	$\frac{1}{2} \left( 2 - a \frac{\sin(kd/2)}{kd/2} - b \cos(kd) \right)$	$\frac{1}{2} \left( a \frac{\sin(kd/2)}{kd/2} - b \right)$
no delay	$\frac{1}{2} \left( 2 - a \frac{\sin(kd/2)}{kd/2} - b \cos(kd/2) \right)$	$\frac{1}{2} \left( a \frac{\sin(kd/2)}{kd/2} - b \cos(kd/2) \right)$

(B1)

## Condition for unidirectionality

If it is required that *the actuator will not radiate sound upstream*, the following equation must be satisfied

Delay optimized:		
downstream	$a \frac{\sin(kd / 2)}{kd / 2} = b \cos(kd)$	
upstream	$a \frac{\sin(kd / 2)}{kd / 2} = b$	(B2)
no delay	$a \frac{\sin(kd / 2)}{kd / 2} = b \cos(kd / 2)$	

In this case the total sound downstream will be

Delay:	$\frac{p_+}{p_i e^{-jkx}} =$	
delay optimized	$1 - b \cos^2(kd / 2)$	(B3)
no delay	$1 - b \cos(kd / 2)$	

## Condition for total cancellation downstream

If it is required that the *total sound pressure downstream will vanish*, the following equation must be satisfied

Delay optimized:		
downstream	$a \frac{\sin(kd/2)}{kd/2} + b = 2$	
upstream	$a \frac{\sin(kd/2)}{kd/2} + b \cos(kd) = 2$	(B4)
no delay	$a \frac{\sin(kd/2)}{kd/2} + b \cos(kd/2) = 2$	

In this case the sound radiation of the actuator upstream will be

Delay:	$\frac{p_-}{p_i e^{+jkx}} =$	
delay optimized	$1 - b \cos^2(kd/2)$	(B5)
no delay	$1 - b \cos(kd/2)$	

## Effort of the actuator

The squared sum of the absolute values of the volume velocities can be written in the case of vanishing sound pressure downstream, using equation (B4), as

Delay optimized:	$\sum_k  q_k ^2 =$	
downstream	$\frac{1}{8} \left( 4 \operatorname{Re}\{b\} -  b ^2 + \frac{4 - 4 \operatorname{Re}\{b\} +  b ^2}{\sin^2(kd/2)} \right)  q_i ^2$	
upstream	$\frac{1}{8} \left(  b ^2 - 4 \operatorname{Re}\{b\} + \frac{4 - 4 \operatorname{Re}\{b\} \cos(kd) +  b ^2 \cos^2(kd)}{\sin^2(kd/2)} \right)  q_i ^2$	(B6)
no delay	$\frac{1}{8} \left(  b ^2 + \frac{4 - 4 \operatorname{Re}\{b\} \cos(kd/2) +  b ^2 \cos^2(kd/2)}{\sin^2(kd/2)} \right)  q_i ^2$	

If the derivatives of this expression attached to variables  $\operatorname{Re}\{b\}$  and  $\operatorname{Im}\{b\}$  are required to vanish, one obtains for the weightings of the *maximally efficient two-element source*.

## Limiting value conditions

If it is required that the *radiation upstream will not exceed a limiting value*

$$|p_-| \leq \frac{|p_i|}{c_1}, \quad (\text{B7})$$

the weightings must obey

Delay optimized:	$\frac{2}{c_1} \geq$	
downstream	$\left  a \frac{\sin(kd/2)}{kd/2} - b \cos(kd) \right $	
upstream	$\left  a \frac{\sin(kd/2)}{kd/2} - b \right $	(B8)
no delay	$\left  a \frac{\sin(kd/2)}{kd/2} - b \cos(kd/2) \right $	

If it is required that the total sound downstream will not exceed a limiting value

$$|p_+| \leq \frac{|p_i|}{c_2}, \quad (\text{B9})$$

the weightings must obey

Delay optimized:	$\frac{2}{c_2} \geq$	
downstream	$\left  2 - a \frac{\sin(kd/2)}{kd/2} - b \right $	
upstream	$\left  2 - a \frac{\sin(kd/2)}{kd/2} - b \cos(kd) \right $	(B10)
no delay	$\left  2 - a \frac{\sin(kd/2)}{kd/2} - b \cos(kd/2) \right $	

## Ratio condition

If there is a requirement for the *ratio of the upstream and downstream sound pressures*

$$\frac{p_- e^{-jkx}}{p_+ e^{+jkx}} = c , \quad (\text{B11})$$

the relation between the weightings  $a$  and  $b$  can be written, according to equation (B1), as

Delay optimized:	$2c =$	
downstream	$a(1+c) \frac{\sin(kd/2)}{kd/2} - b(\cos(kd) - c)$	
upstream	$a(1+c) \frac{\sin(kd/2)}{kd/2} - b(1 - c \cos(kd))$	(B12)
no delay	$a(1+c) \frac{\sin(kd/2)}{kd/2} - b(1-c) \cos(kd/2)$	

This kind of requirement may be useful when optimizing the total efficiency of a detector-actuator system. The optimum value of the ratio for the actuator depends on the directional characteristics of the detector (how sensitive the detector is to the acoustic feedback).

In this case the total sound pressure downstream and the sound pressure upstream are

Delay:	$\frac{p_+}{p_i e^{-jkx}} =$	$\frac{p_-}{p_i e^{+jkx}} =$	
delay optimized	$\frac{1}{1+c} [1 - b \cos^2(kd/2)]$	$\frac{c}{1+c} [1 - b \cos^2(kd/2)]$	(B13)
no delay	$\frac{1}{1+c} [1 - b \cos(kd/2)]$	$\frac{c}{1+c} [1 - b \cos(kd/2)]$	

If the monopole is not modified ( $b = 1$ ), according to equation (B12) weighting  $a$  can be written as

Delay optimized:	$a =$	
downstream	$\frac{c + \cos(kd)}{1+c} \frac{kd/2}{\sin(kd/2)}$	
upstream	$\frac{1+c(2 - \cos(kd))}{1+c} \frac{kd/2}{\sin(kd/2)}$	(B14)
no delay	$\frac{2c + (1-c) \cos(kd/2)}{1+c} \frac{kd/2}{\sin(kd/2)}$	

The total sound pressure downstream and the sound pressure upstream are as in equation (B13), and can also be presented as

Delay:	$\frac{p_+}{p_i e^{-jkx}} =$	$\frac{p_-}{p_i e^{+jkx}} =$	
delay optimized	$\frac{1}{1+c} \sin^2(kd/2)$	$\frac{c}{1+c} \sin^2(kd/2)$	(B15)
no delay	$\frac{1}{1+c} (1 - \cos(kd/2))$	$\frac{c}{1+c} (1 - \cos(kd/2))$	

If the dipole is not modified ( $a = 1$ ), according to equation (B12) weighting  $b$  can be written as

Delay optimized:	$b =$	
downstream	$\frac{1}{\cos(kd) - c} \left( (1+c) \frac{\sin(kd/2)}{kd/2} - 2c \right)$	(B16)
upstream	$\frac{1}{1 - c \cos(kd)} \left( (1+c) \frac{\sin(kd/2)}{kd/2} - 2c \right)$	
no delay	$\frac{1}{(1-c) \cos(kd/2)} \left( (1+c) \frac{\sin(kd/2)}{kd/2} - 2c \right)$	

The total sound pressure downstream and the sound pressure upstream are the same as in equation (B13), and can also be presented as

Delay optimized:	$\frac{P_+}{p_i e^{-jkx}} =$	$\frac{P_-}{p_i e^{+jkx}} =$
down-stream	$\frac{1}{\cos(kd) - c} \left( \cos(kd) - \cos^2(kd/2) \frac{\sin(kd/2)}{kd/2} \right)$	$\frac{c}{\cos(kd) - c} \left( \cos(kd) - \cos^2(kd/2) \frac{\sin(kd/2)}{kd/2} \right)$
upstream	$\frac{1}{1 - c \cos(kd)} \left( 1 - \frac{\sin(kd/2)}{kd/2} \cos^2(kd/2) \right)$	$\frac{c}{1 - c \cos(kd)} \left( 1 - \frac{\sin(kd/2)}{kd/2} \cos^2(kd/2) \right)$
no delay	$\frac{1}{1 - c} \left( 1 - \frac{\sin(kd/2)}{kd/2} \right)$	$\frac{c}{1 - c} \left( 1 - \frac{\sin(kd/2)}{kd/2} \right)$

(B17)